Regulation of Skn7-dependent, oxidative stress-induced genes by the RNA polymerase II-CTD phosphatase, Fcp1, and Mediator kinase subunit, Cdk8, in yeast

Received for publication, March 28, 2019, and in revised form, August 23, 2019 Published, Papers in Press, September 10, 2019, DOI 10.1074/jbc.RA119.008515

Maria J. Aristizabal[‡§¶], Kristy Dever[‡], Gian Luca Negri[‖], Mary Shen[‡], Nicole Hawe[**], Joris J. Benschop[‡‡], Frank C. P. Holstege[‡‡], Nevan J. Krogan[§§], Ivan Sadowski[**], and Michael S. Kobor[‡1]

*From the [‡]Centre for Molecular Medicine and Therapeutics, BC Children's Hospital Research Institute, Department of Medical Genetics, University of British Columbia, Vancouver, British Columbia V5Z 4H4, Canada, the [§]Department of Ecology and Evolutionary Biology, University of Toronto, Toronto, Ontario M5S 3B2, Canada, the [¶]Child and Brain Development Program, Canadian Institute for Advanced Research (CIFAR), Toronto, Ontario M5G 1Z8, Canada, [‖]Canada's Michael Smith Genome Sciences Centre, BC Cancer, Vancouver V5Z 1L3, British Columbia, Canada, the **Department of Biochemistry and Molecular Biology, Molecular Epigenetics, Life Sciences Institute, University of British Columbia, Vancouver V6T 1Z3, British Columbia, Canada, the [‡‡]Princess Máxima Center for Pediatric Oncology, Heidelberglaan 25, 3584 CS Utrecht, The Netherlands, and the [§§]Department of Cellular and Molecular Pharmacology, University of California, San Francisco, California 94158*

Edited by Joel M. Gottesfeld

Fcp1 is a protein phosphatase that facilitates transcription elongation and termination by dephosphorylating the C-terminal domain of RNA polymerase II. High-throughput genetic screening and gene expression profiling of *fcp1* mutants revealed a novel connection to Cdk8, the Mediator complex kinase subunit, and Skn7, a key transcription factor in the oxidative stress response pathway. Briefly, Skn7 was enriched as a regulator of genes whose mRNA levels were altered in *fcp1* and *cdk8*Δ mutants and was required for the suppression of *fcp1* mutant growth defects by loss of *CDK8* under oxidative stress conditions. Targeted analysis revealed that mutating *FCP1* decreased Skn7 mRNA and protein levels as well as its association with target gene promoters but paradoxically increased the mRNA levels of Skn7-dependent oxidative stress-induced genes (*TRX2* and *TSA1*) under basal and induced conditions. The latter was in part recapitulated via chemical inhibition of transcription in WT cells, suggesting that a combination of transcriptional and posttranscriptional effects underscored the increased mRNA levels of *TRX2* and *TSA1* observed in the *fcp1* mutant. Interestingly, loss of *CDK8* robustly normalized the mRNA levels of Skn7-dependent genes in the *fcp1* mutant background and also increased Skn7 protein levels by preventing its turnover. As such, our work suggested that loss of *CDK8* could overcome transcriptional and/or posttranscriptional alterations in the *fcp1* mutant through its regulatory effect on Skn7. Furthermore, our work also implicated *FCP1* and *CDK8* in the broader response to environmental stressors in yeast.

In eukaryotes, RNA polymerase II (RNAPII)[2] is the enzyme responsible for transcribing all protein-coding genes. Its largest subunit contains a highly conserved C-terminal domain (CTD) composed of heptapeptide repeats (Tyr1-Ser2-Pro3-Thr4-Ser5-Pro6-Ser7) that is essential for viability (1–3). The CTD is differentially phosphorylated throughout the transcription cycle, with each transcriptional stage characterized by a unique phosphorylation signature and the recruitment of specific regulatory, RNA-processing, and chromatin-remodeling factors (4). As such, a number of kinases (Kin28, Ctk1, Bur1, and Cdk8) and phosphatases (Fcp1, Rtr1, Ssu72, and Glc7) play key roles in transcription regulation (5).

Fcp1 (TFIIF-associating CTD phosphatase 1) was the first RNAPII-CTD phosphatase identified (6), encoded by a conserved gene that is essential for viability (7, 8). It contains a catalytic FCP homology (FCPH) domain and a single BRCA1 C-terminal (BRCT) domain, both of which are important for activity (9, 10). The latter mediates direct contacts with the RNAPII-CTD (9, 11), although its exact role within Fcp1 remains enigmatic. Functionally, Fcp1 associates along the length of genes and facilitates transcription elongation and recycling by dephosphorylating Ser^2 and Thr^4 residues on the RNAPII-CTD (12–15). Underscoring the significance of Fcp1 in facilitating transcription, temperature-sensitive *fcp1* mutants that target the catalytic domain result in the accumulation of hyperphosphorylated RNAPII and a global shutdown of transcription at nonpermissive temperatures (6, 13, 14).

This work was supported by Natural Sciences and Engineering Research Council of Canada (NSERC) Grant RPGIN-2016–04297 (to M. S. K.), a PDF fellowship (to M. J. A.), and a USRA studentship (to M. S.). The authors declare that they have no conflicts of interest with the contents of this article.

This article contains Figs. S1–S6.

Microarray data were submitted to the Gene Expression Omnibus under accession number GSE128936.

[1] To whom correspondence should be addressed: Centre for Molecular Medicine and Therapeutics, 950 West 28th Ave., Vancouver, British Columbia V5Z 4H4, Canada. Tel.: 604-875-3803; Fax: 604-875-3819; E-mail: msk@bcchr.ca.

[2] The abbreviations used are: RNAPII, RNA polymerase II; CTD, C-terminal domain; FCPH, FCP-homology domain; BRCT, BRCA1 C terminus domain; TFIIF and TFIIB, general transcription factor IIF and IIB, respectively; MMS, methyl methanesulfonate; HU, hydroxyurea; E-MAP, epistasis mini-assay profiling; TF, transcription factor; qPCR, quantitative PCR; HA, hemagglutinin; OD, optical density; IP, immunoprecipitation; KLB, kinase lysis buffer; TAP, tandem affinity purification; IQR, interquantile range.

Despite its importance, the full extent of Fcp1 function in the cell, as well as the exact mechanisms controlling its activity and recruitment to sites of transcription, remains poorly understood. Nevertheless, a subset of factors, including the general transcription factors TFIIF and TFIIB, have been implicated in the regulation of Fcp1 activity (7, 10, 14, 16–21). Furthermore, recent studies have ascribed Fcp1 roles beyond the RNAPII-CTD. For instance, in fission yeast, Fcp1 can dephosphorylate Spt5 (22); in mammals, mitotic exit factors (Wee1, Cdc20, USP44, Ensa and Greatwall) (23–25); and in budding yeast and mammals, RNAPI transcription initiation factors (Rrn3 and TIF-IA, respectively) (26, 27). Together, these findings are consistent with evidence positioning *FCP1* earlier in evolutionary history than the gene encoding its best-known substrate, the RNAPII-CTD (28).

To better-understand the role of Fcp1 in the cell, high-throughput gene expression and genetic interaction profiling was performed on a series of *fcp1* mutants, leading us to uncover a role in the response to environmental stress that was linked to *CDK8,* encoding the Mediator complex kinase subunit. In brief, the *fcp1-594* mutant was sensitive to oxidative stress and had altered regulation of Skn7, a key transcription factor in the oxidative stress response, defects that were normalized by loss of *CDK8*. Strikingly, the *fcp1-594* mutant had elevated mRNA levels of Skn7-dependent oxidative stress–responsive genes (*TSA1* and *TRX2*) under basal and inducing conditions, an effect dependent on the kinase activity of Cdk8. Collectively, our work suggested that loss of *CDK8* could overcome the transcriptional and posttranscriptional alterations of the *fcp1* mutant by increasing Skn7 stability, protein levels, and likely the expression of target genes. In addition, our results also implicate *FCP1* and *CDK8* in the response to other environmental stressors, laying the foundation for future investigations.

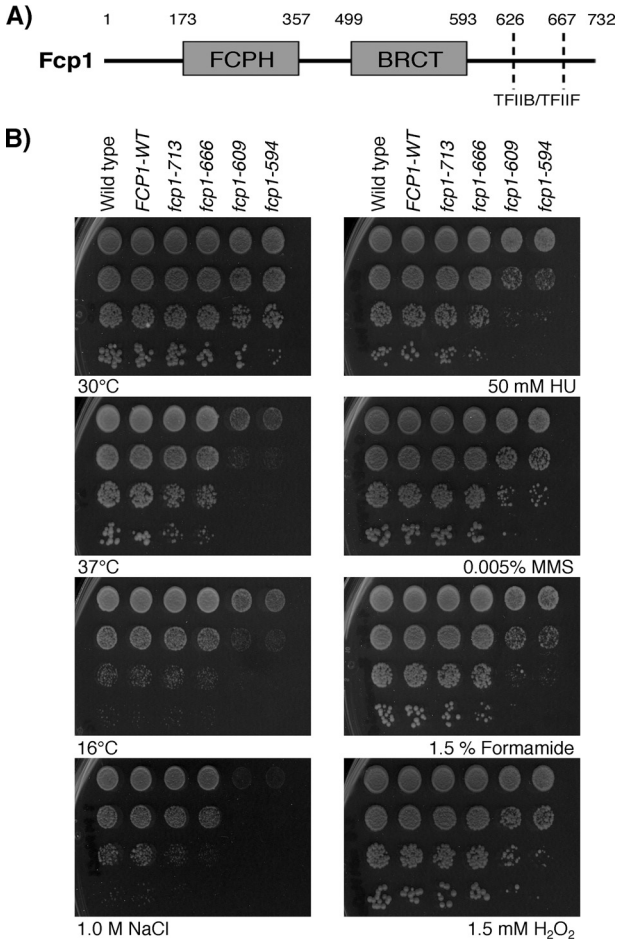

Figure 1. *FCP1* mutants were sensitive to genotoxic agents and environmental stressors. *A*, *schematic* of *FCP1* illustrating the FCPH catalytic domain, BRCT domain, and TFIIF/TFIIB-interacting region. The *FCP1* mutants differentially removed the TFIIF/TFIIB-binding regions. *B*, the two shortest *FCP1* mutants were sensitive to high (37 °C) and low (16 °C) temperatures and the indicated concentrations of hydroxyurea, methyl methanesulfonate, sodium chloride (NaCl; osmotic stress), and hydrogen peroxide (H_2O_2; oxidative stress). Cells with the indicated mutations were serially diluted 10-fold, spotted on YPD media with the indicated drug concentrations, and grown for 2–4 days.

Results

Gene expression profiles of FCP1 mutants suggested a role in the response to stress and a relationship with the gene encoding the Mediator complex kinase subunit, CDK8

To better understand the role of *FCP1* in the cell, a set of *fcp1* mutants (*FCP1-WT, fcp1-713*, *fcp1-666*, *fcp1-609*, *fcp1-594*, which result in the production of C-terminally truncated Fcp1 proteins) were generated at the endogenous *FCP1* locus and exposed to a variety of genotoxic agents and stress conditions (Fig. 1, *A* and *B*). These truncation alleles were described previously, and their protein products were shown to differentially disrupt the interaction with TFIIF and TFIIB while leaving the rest of Fcp1 intact (8, 10). Suggestive of a general function in the response to stress, the two shortest truncation mutants (*fcp1-594* and *fcp1-609*) exhibited fitness defects when grown at high (37 °C) or low temperatures (16 °C) or exposed to hydroxyurea (HU), methyl methanesulfonate (MMS), formamide, osmotic stress (NaCl), or oxidative stress (H_2O_2) conditions (Fig. 1*B*). The longer *fcp1-666* mutant showed an intermediate phenotype and was only sensitive to formamide and HU, whereas the *fcp1-713* mutant and the *FCP1-WT* strain produced no growth defects.

Having observed a range of fitness defects, we next determined whether these correlated with transcriptional defects. Gene expression profiles were generated using microarrays and compared with the isogenic control strain (*FCP1-WT*). Perhaps not surprisingly, the deletion mutants displayed milder gene expression alterations than two previously described and more severe *FCP1* alleles, *fcp1-1* and *fcp1-2* (encoding Fcp1 R250A/R251A and L117A/L181A/H187A, respectively), which target the FCPH catalytic domain and result in a global shutdown of transcription at nonpermissive temperatures (6). Nevertheless, our gene expression profiles revealed length-dependent requirements, with the severity and number of transcriptional alterations generally increasing as the C terminus was progressively shortened (Fig. 2, *A* and *B*). However, we note that the *fcp1-609* mutant, rather than the shortest *fcp1-594* mutant had the greatest number of transcriptional alterations (Fig. 2*C*), suggesting a nuanced role for the *FCP1* C terminus in transcription regulation. Despite the noted differences, there was a significant overlap between the *fcp1-594* and *fcp1-609* mutant expression profiles, allowing us to focus on genes whose expression was altered in both mutants (67 genes with decreased mRNA levels and 22 genes with increased mRNA levels), thus

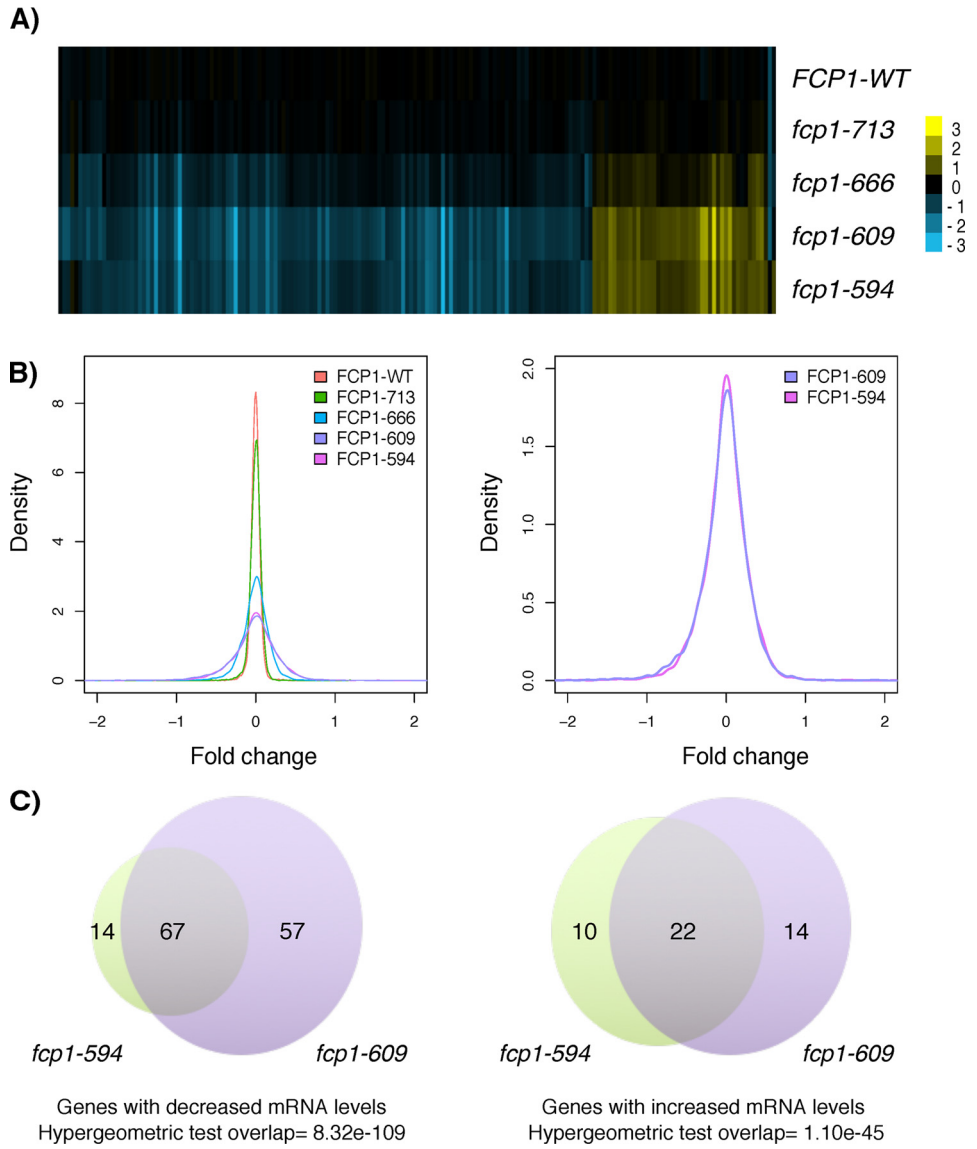

Figure 2. The *fcp1-594* and *fcp1-609* mutants resulted in an overlapping set of gene expression alterations. *A*, heat map of mRNA levels showing genes differentially expressed ($p < 0.01$ and -fold change > 1.7) in the *fcp1-594* or *fcp1-609* mutant. *Yellow*, increased mRNA levels compared with WT; *blue*, decreased levels. *B*, *left*, distribution of gene expression -fold changes for the *FCP1* mutants showed a length-dependent effect on gene expression. *Right*, focusing on the shortest mutants revealed that the *fcp1-609* and not the shortest *fcp1-594* mutant had the greatest number of gene expression defects. *C*, Venn diagram of genes differentially expressed in the *fcp1-609* and *fcp1-594* mutant showed a significant overlap (hypergeometric test, $p < 0.01$) as well as a high degree of gene-specific effects.

increasing confidence in our findings. Focusing on this gene set, we performed transcription factor (TF) enrichment analysis using the Yeast Promoter Atlas (29). This analysis revealed that the *fcp1*-dependent genes were enriched for regulation by TFs previously implicated in the response to stress (Mcm1, Ste12, Phd1, Sok2, Skn7, Sko1, Hot1, Bas1, and Cad1) (Fig. 3*A*), consistent with the *fcp1* mutants showing growth defects across a variety of stress conditions. Follow-up targeted analysis confirmed a role for *FCP1* in the regulation of a representative set of these TFs; the *fcp1-594* mutant had decreased *SKN7*, *SOK2*, and *MCM1* mRNA levels and Skn7, Sok2, Mcm1 and Cad1 protein levels (Fig. 3, *B–E*).

Strikingly, the list of enriched TFs included two well-known substrates of the Mediator complex kinase subunit, Cdk8 (Ste12 and Phd1 (30, 31)) as well as the Phd1 ohnolog, Sok2 (32). This suggested relationship to *CDK8* was further supported by a significant overlap in the TFs enriched for regulating genes whose mRNA levels were altered in the *fcp1-594* and *609* mutants and those altered upon loss of *CDK8* (seven of nine TFs, hypergeometric test, $p = 0.0008035$) (Fig. 3*A* (TFs marked with an *asterisk*) and Fig. S1*A*). Markedly, whereas the overlapping TFs associated with genes whose mRNA levels decreased in the *FCP1* mutants (Fig. 3*A*, *light gray bars*), they related to genes whose mRNA levels increased in the *cdk8*Δ mutant (Fig. S1*A*, *dark gray bars*), indicating possible opposite effects on the regulation of these TFs (*cdk8*Δ mutant expression profile obtained from Ref. 33). To further explore the relationship of Cdk8 with these TFs, we examined available Cdk8 genome localizations derived from ChIP-chip profiles and found that Cdk8 physically associated with the promoters of a subset of genes regulated by the TFs from our analysis (Cdk8 ChIP-chip profile obtained from Ref. 34) (Fig. S1*B*). Finally, linking

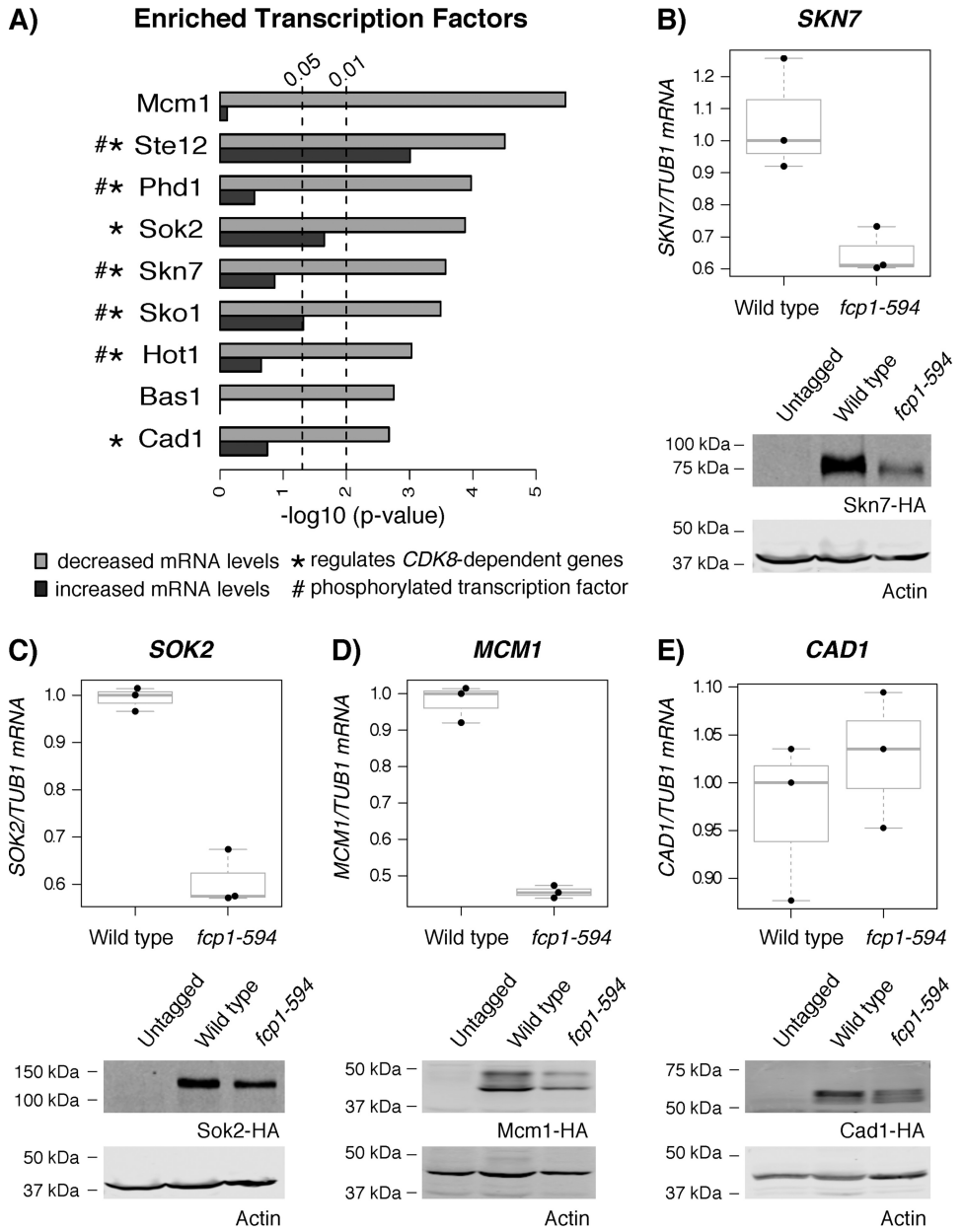

Figure 3. *FCP1* played a role in regulating the mRNA and protein levels of a subset of TFs. *A*, TFs enriched for regulating genes differentially expressed in the *fcp1-594* and *fcp1-609* mutant. *Light gray bars*, enrichment of TFs for genes whose mRNA levels decreased in the *fcp1-594* and *fcp1-609* mutant; *dark gray boxes*, enrichment for genes whose mRNA levels increased in the *fcp1-594* and *fcp1-609* mutant. Most enriched transcription factors significantly associated ($p < 0.01$) with genes whose mRNA levels decreased in the *fcp1-594* and *fcp1-609* mutant, with the exception of Ste12, which also showed a significant association with genes whose mRNA levels increased. A significant number of TFs also regulated genes whose mRNA levels are altered upon loss of *CDK8* (hypergeometric test, $p < 0.01$ (*)) and had strong evidence of being phosphorylated proteins (hypergeometric test, $p = 0.03769$ (#)). *B–E*, *top*, the *fcp1-594* mutant reduced *SKN7*, *SOK2*, and *MCM1* mRNA levels but had no effect on *CAD1*. mRNA levels were normalized to *TUB1* (75). mRNA levels are shown as *box plots* displaying the median and interquartile range, with *whiskers* denoting 1.5 times the interquartile range. *Bottom*, immunoblots of Skn7, Sok2, Mcm1, and Cad1 protein levels showed decreased levels in the *fcp1-594* mutant compared with WT. Actin was used as a loading control.

these TFs with a protein kinase and phosphatase, respectively, was intriguing, as it raised the possibility that the TFs were regulated by phosphorylation. Using the Yeast Kinase Interaction Database (35), we found a significant enrichment for proteins with strong evidence (score >6.4) of being phosphorylated in this small set of TFs (hypergeometric test, $p = 0.03769$) (Fig. 3*A*, TFs marked with a *number symbol*), which suggested a role for *FCP1* and *CDK8* in the biology of stress response TFs, perhaps through effects on their phosphorylation state.

The genetic interaction network of the FCP1 mutants supported a role in the regulation of SKN7 and SOK2

To gain insight into the cellular processes and pathways influenced by *FCP1*, the *fcp1* truncation mutants described above were screened against a library of 1536 different mutants involved in chromatin biology, transcription, and RNA processing using epistasis miniarray profiling (E-MAP) (36). Overall, the genetic interaction profiles revealed similar functional information as the gene expression profiles (Fig. 4*A*). They showed that the number and strength of genetic interactions

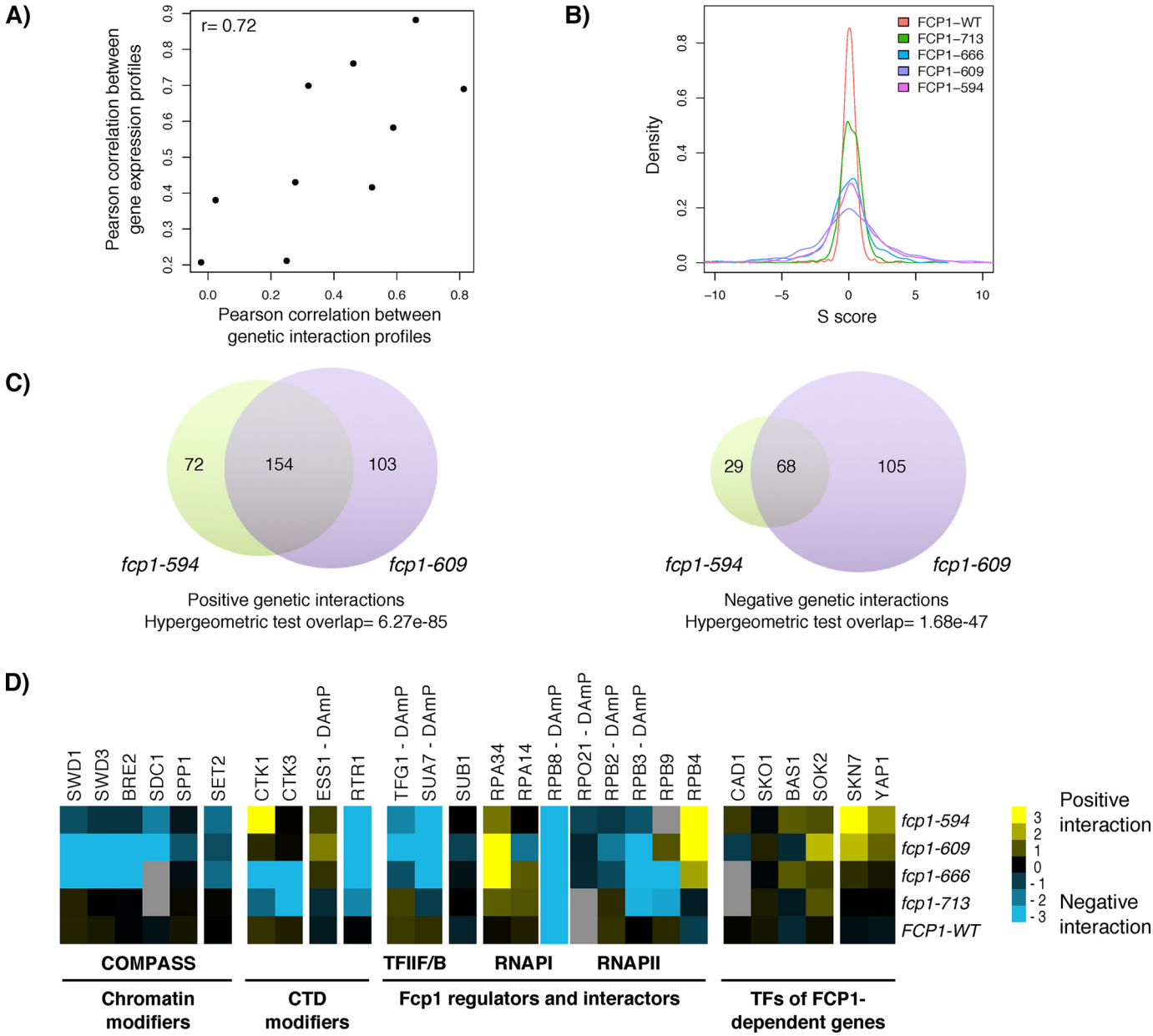

Figure 4. Genetic interaction profiles of *FCP1* mutants were consistent with its function as an RNAPII-CTD phosphatase and supported a role in transcription factor biology. *A*, the genetic and gene expression profiles revealed similar relationships across the various *FCP1* mutants. The scatter plot of profile-paired correlations of the genetic interaction and gene expression profiles revealed a high correlation (0.72). *B*, distribution of *S* scores for the *FCP1* mutants showed that the *fcp1-609* mutant had the greatest number of significant genetic interactions. The *S* score is a modified *T*-statistic that captures the significance and strength of the genetic interaction. *S* scores greater than 2 and less than −2.5 were considered significant. *C*, Venn diagrams comparing the significant genetic interactions of the *fcp1-609* and *fcp1-594* mutants. Whereas the overlap in genetic interactions was significant (hypergeometric test, $p < 0.01$), there were also several genetic interactions that were unique to each mutant. *D*, subset of genetic interactions for the *FCP1* mutants showed significant interactions with *SOK2* and *SKN7*. Each mutant was screened in triplicate, with *yellow*, *blue*, and *gray* indicating alleviating, aggravating, and missing values, respectively.

increased as Fcp1 protein was progressively shortened from the C terminus (Fig. 4*B*) and that the *fcp1-609* mutant, and not the shortest *fcp1-594* mutant, had the greatest number of genetic interactions (Fig. 4*C*). Furthermore, these profiles were consistent with known Fcp1 functions, including its role as an RNAPII-CTD phosphatase. For instance, they showed length-dependent genetic interactions with TFIIF and TFIIB, consistent with the differential effects of truncated Fcp1 mutant proteins on the physical interaction with both of these general transcription factors (10). This analysis also revealed significant genetic interactions with genes encoding RNAPII-CTD–modifying enzymes (*CKT1*, *ESS1*, and *RTR1*) (13, 37–40) (Fig. 4*D*) and genes encoding factors that bind the RNAPII-CTD in a phosphorylation-dependent manner, including members of the Set1-containing H3K4 methyltransferase COMPASS complex (41). Finally, the *FCP1* genetic interaction profiles supported a functional relationship with the TFs identified by the gene expression analysis. Notably, both the *fcp1-594* and *fcp1-609* mutants showed strong positive interactions with *SOK2* and *SKN7* (Fig. 4*D*), with a link to *SKN7* further supported by a positive interaction between the *fcp1-594* and *fcp1-609* mutants with *YAP1*, a transcription factor partner of Skn7 (42).

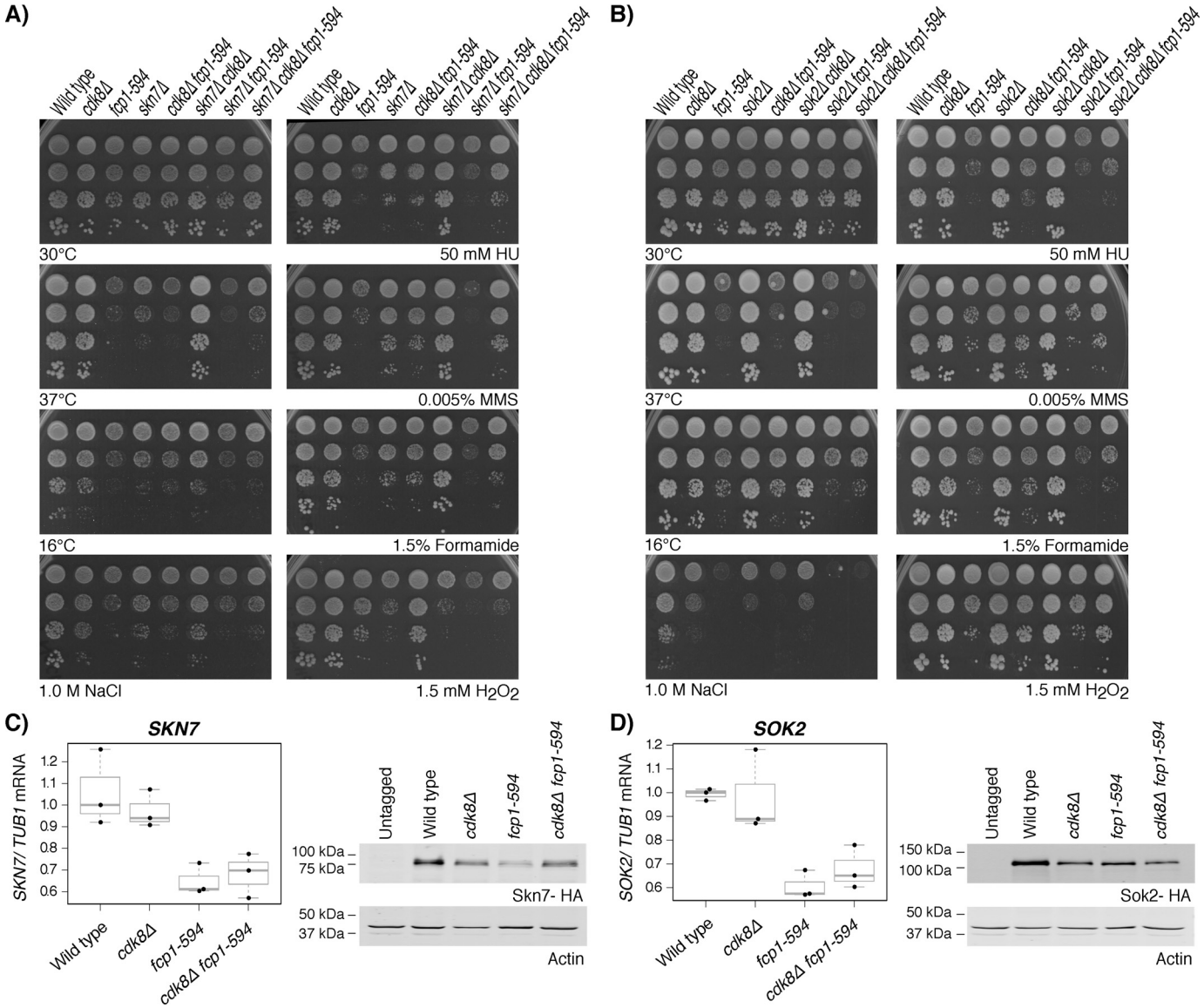

Figure 5. Loss of *CDK8* suppressed *fcp1-594* and *skn7*Δ mutant growth defects. Shown is the sensitivity of *cdk8*Δ, *fcp1-594*, and either *skn7*Δ (*A*) or *sok2*Δ (*B*) single, double, and triple mutants to growth under high (37 °C) and low (16 °C) temperatures, and upon exposure to the indicated concentrations of H_2O_2, NaCl, hydroxyurea, formamide, and methyl methanesulfonate. Loss of *CDK8* suppressed the growth defects of both the *fcp1-594* and *skn7*Δ single mutants, suggesting a shared function. Shown are RT-qPCR measurements (*left*) of *SKN7* (*C*) and *SOK2* (*D*) mRNA levels in WT or the indicated mutants normalized to *TUB1* (75). mRNA levels are shown as *box plots* displaying the median and interquartile range, with *whiskers* denoting 1.5 times the interquartile range. Immunoblotting (*right*) of Skn7 (*C*) and Sok2 (*D*) bulk protein levels revealed that loss of *CDK8* increased Skn7 protein levels in the *fcp1-594* mutant background. Extracts were prepared from the indicated strains, and actin was used as a loading control.

Loss of CDK8 suppressed phenotypes associated with the fcp1-594 and skn7Δ mutant

Collectively, our high-throughput data suggested a link between *FCP1* and *CDK8* in *SKN7* and *SOK2* function. To explore this relationship further, single, double, and triple mutants of *fcp1-594*, *cdk8*Δ and either *skn7*Δ or *sok2*Δ were generated, and their phenotypes were analyzed by measuring growth under the conditions described above (Fig. 5, *A* and *B*). Under these conditions, the *cdk8*Δ mutant generally produced phenotypes typical of the WT strain, whereas the *skn7*Δ mutant was sensitive to most of the conditions tested, including high temperature, H_2O_2, and NaCl, effects consistent with known roles for Skn7 (Fig. 5*A*) (43–45). Interestingly, across most conditions tested, loss of *CDK8* suppressed the *fcp1-594* and *skn7*Δ mutant growth defects, underscoring a functional relationship. We note that the suppression of *skn7*Δ mutant phenotypes by loss of *CDK8* required *FCP1*. In contrast, the suppression of *fcp1-594* mutant phenotypes by loss of *CDK8* was generally independent of *SKN7*, indicating that a functional relationship between *FCP1* and *CDK8* likely involved multiple pathways, some of which are independent of *SKN7*. A notable exception to this pattern was observed under oxidative stress conditions, wherein suppression of *fcp1-594* mutant phenotypes by loss of *CDK8* required *SKN7*. In contrast, the *sok2*Δ mutant showed little or no sensitivity to all of the conditions examined (Fig. 5*B*), indicating minimal genetic relationship with *FCP1* and/or *CDK8*.

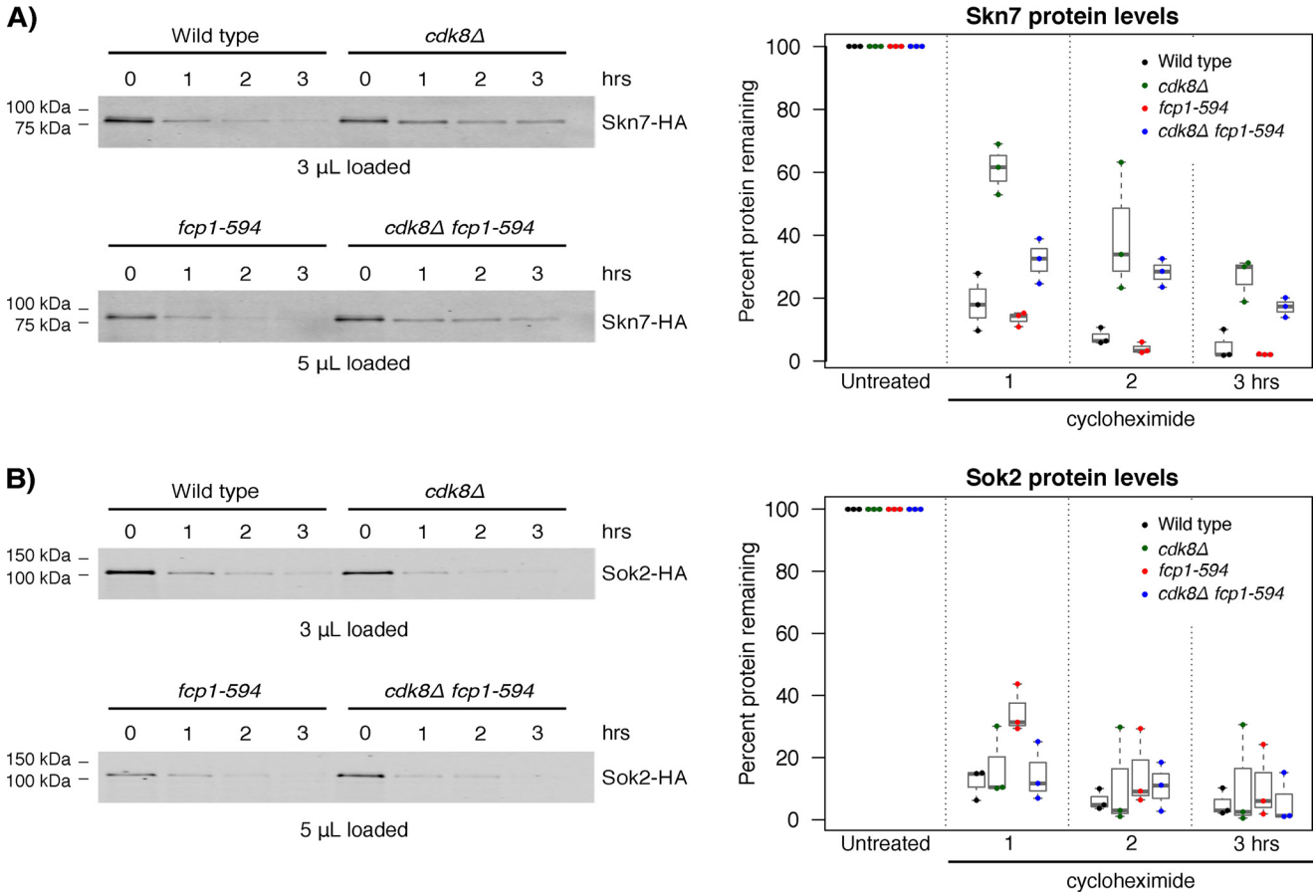

Figure 6. *CDK8* and *FCP1* altered Skn7 protein stability. *Left*, representative immunoblots of Skn7 (*A*) or Sok2 (*B*) protein levels before and after inhibition of protein synthesis by the addition of 100 μg/ml cycloheximide. As indicated, protein loading was adjusted in the *fcp1-594* and *fcp1-594 cdk8*Δ mutant with the goal of having similar starting protein amounts. *Right*, quantification of Skn7 (*A*) or Sok2 (*B*) immunoblots with protein levels expressed as a percentage of the untreated control. Loss of *CDK8* stabilized Skn7 protein levels *in vivo*. Normalized protein levels are shown as *box plots* displaying the median and interquartile range, with *whiskers* denoting 1.5 times the interquartile range.

To gain further insight into the relationship between *FCP1* and *CDK8* in *SKN7* or *SOK2* function, we next examined how these factors affected their mRNA and/or protein levels. As described above, the *fcp1-594* mutant decreased the mRNA and protein levels of both *SKN7* and *SOK2*, an effect that differed from the *cdk8*Δ mutant strain, which showed decreased protein levels of both TFs but no effects on their mRNA levels (Fig. 5, *C* and *D*). Consistent with the genetic dependences described above, loss of *CDK8* alleviated the decreased Skn7 protein levels observed in the *fcp1-594* mutant, although it did not alter Sok2 protein levels or the mRNA levels of either of these TFs. Finally, we note that the effects of *FCP1* and *CDK8* on Skn7 were specific, given that the trends described above were not observed on the mRNA or protein levels of Yap1, Skn7's intimate functional partner (Fig. S2).

Altered CDK8 and FCP1 function led to changes in Skn7 protein stability

The discrepancy between *SKN7* and *SOK2* mRNA and protein levels observed in the *cdk8*Δ mutant suggested that *CDK8* might affect Skn7 and or Sok2 protein stability, an effect reminiscent of *CDK8*'s well-known role in phosphorylating and destabilizing Ste12, Phd1, and Gcn4 (30, 31, 46). Taking advantage of the ability to inhibit protein synthesis using cycloheximide, we measured Skn7 and Sok2 stability in WT and the *fcp1-594* and *cdk8*Δ single and double mutants. Under WT conditions, Skn7 and Sok2 were almost completely degraded 3 h after blocking protein production, leading to estimates of half-life for both TFs at roughly 30 min (Fig. 6, *A* and *B*). Strikingly, in the *cdk8*Δ mutant, Skn7 protein levels decayed at a slower rate, revealing a role for *CDK8* in Skn7 protein turnover. In contrast, the *fcp1-594* mutant on its own had no effect on Skn7 protein turnover, but when combined with the *cdk8*Δ mutant, it decreased Skn7 protein stability to a level between the WT and *cdk8*Δ mutant, an effect most noticeable 1 and 3 h after inhibition of protein synthesis. As such, our results suggested that *CDK8* promoted Skn7 turnover in a manner that was partly dependent on *FCP1*. Finally, no effects of the *fcp1-594* or *cdk8*Δ mutants were seen on Sok2 protein stability; thus, it was not explored further.

CDK8 and FCP1 regulated Skn7 phosphorylation

A role for *CDK8* and *FCP1* on Skn7 protein stability prompted us to determine whether this involved an effect on Skn7 phosphorylation *in vivo*. In the WT strain, treatment of Skn7, purified by immunoprecipitation, with λ-phosphatase resulted in faster migration compared with untreated or λ-phosphatase plus inhibitor–treated samples, indicating that

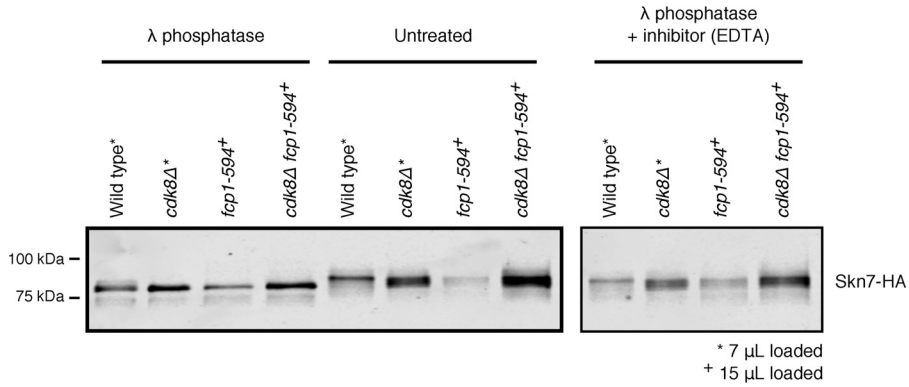

Figure 7. Phosphorylation of Skn7 depended on *CDK8* and *FCP1*. Skn7 purified by immunoprecipitation was untreated or treated with 200 units of λ-phosphatase for 1 h in the presence or absence of 100 mM EDTA inhibitor, as indicated. Slower Skn7 migration was observed in untreated samples and in samples treated with λ-phosphatase plus EDTA phosphatase inhibitor, indicating the presence of phosphorylation. Reduced but not completely abolished phosphorylation was observed in the *fcp1-594*, *cdk8*Δ, and *fcp1-594 cdk8*Δ mutants compared with WT. Protein loading was adjusted as indicated.

Skn7 was generally phosphorylated under normal growth conditions, consistent with previous reports (Fig. 7) (42). In the *fcp1-594* and *cdk8*Δ single and double mutants, Skn7 migrated as an intermediate species, indicating a role for these enzymes on Skn7 phosphorylation *in vivo*. Observing an intermediate effect for the *cdk8*Δ mutant was consistent with evidence that other kinases are involved in Skn7 phosphorylation (47).

A role for *CDK8* in regulating the levels of Skn7 phosphorylation, combined with previous reports of a direct physical interaction between Cdk8 and Skn7 (48), suggested that Cdk8 may directly phosphorylate Skn7. To test this hypothesis, *in vitro* kinase reactions were performed with recombinant Skn7 as substrate for WT or kinase-inactive Cdk8 (D290A (49)) recovered from yeast by immunoprecipitation. Under these conditions, WT Cdk8, but not the kinase inactive mutant, robustly phosphorylated the RNAPII-CTD, a previously reported substrate (Fig. S3) (49–51). Under the same conditions, we detected no phosphorylation of Skn7 by Cdk8, suggesting that its effect *in vivo* may reflect an indirect mechanism or that Skn7 phosphorylation requires an additional co-factor that is absent from the *in vitro* reactions.

FCP1 and CDK8 functioned in the regulation of Skn7-dependent oxidative stress–responsive genes

The results presented so far revealed a role for *CDK8* and *FCP1* in the regulation of Skn7, leading us to examine whether these factors also functioned in the transcriptional regulation of oxidative stress–responsive genes. To this end, we focused on two representative and well-established Skn7-dependent oxidative stress-induced genes, *TRX2* and *TSA1*, and measured their mRNA levels using RT-qPCR in untreated cells and following exposure to 0.2 mM H_2O_2. Consistent with previous findings, the expression of *TRX2* and *TSA1* was induced in response to oxidant (52, 53), an effect also seen in the *fcp1-594* and *cdk8*Δ single and double mutants (Fig. 8*A*). However, we note that the *fcp1-594* mutant robustly increased the basal and induced mRNA levels of both *TSA1* and *TRX2*, an effect not easily reconcilable with the decreased levels of Skn7 observed in the same strain. Under oxidative stress conditions, the robust increases of *TRX2* and *TSA1* mRNA levels observed in the *fcp1-594* mutant were not a result of bypassing the requirement for *SKN7*, as no increase was observed in a strain carrying a *skn7* deletion in combination with the *fcp1-594* mutant or any of the other mutant backgrounds (Fig. S4*A*). Most interestingly and consistent with shared roles for *FCP1* and *CDK8* in the regulation of Skn7, loss of *CDK8* in an *fcp1-594* mutant background normalized the elevated *TRX2* and *TSA1* mRNA levels observed in the *fcp1-594* mutant under basal and induced conditions (Fig. 8*A* and Fig. S4*B*). Furthermore, the effect of *CDK8* on *TSA1* and *TRX2* mRNA levels depended on its kinase activity, given that introduction of a catalytically inactive *CDK8D290A* allele decreased the induced mRNA levels of *TSA1* and *TRX2* in the *fcp1-594 cdk8*Δ mutant compared with a WT *CDK8* allele (Fig. S4*B*).

The unexpected effect of the *fcp1-594* mutant on the expression of Skn7-dependent genes led us to examine Skn7 protein levels under oxidative stress conditions. Here, we found that oxidative stress recapitulated the observations under normal growth conditions, where the *fcp1-594* mutant showed decreased Skn7 protein levels under basal and oxidative stress conditions that were normalized by loss of *CDK8*. Thus, in the *fcp1-594* mutant, elevated *TSA1* and *TRX2* mRNA levels were dependent on *SKN7*, despite its protein levels being decreased in the *fcp1-594* mutant under basal and oxidative stress conditions.

To understand the discrepancy between Skn7 protein levels and expression of its target genes in the *fcp1-594* mutant, we measured RNAPII and Skn7 occupancy at these loci via ChIP of endogenous Rpb3 and Skn7-FLAG, respectively. Consistent with the increase in *TRX2* and *TSA1* mRNA levels upon exposure to 0.2 mM H_2O_2 and Skn7's role as a transcriptional activator (52, 54), we observed increased RNAPII and Skn7 occupancy at these loci upon treatment in the WT strain, an effect most striking at the *TSA1* locus (Fig. 8*B* and Fig. S5 (*B* and *C*)). For RNAPII, the *fcp1-594* and *cdk8*Δ single and double mutants also showed increased RNAPII occupancy upon exposure to H_2O_2, indicating increased transcription in response to stress. However, we note that whereas the *cdk8*Δ and *fcp1-594 cdk8*Δ mutants tended to increase RNAPII occupancy at the promoter and along the length of *TRX2* and *TSA1*, the *fcp1-594* mutant showed a more pronounced effect along the length of these

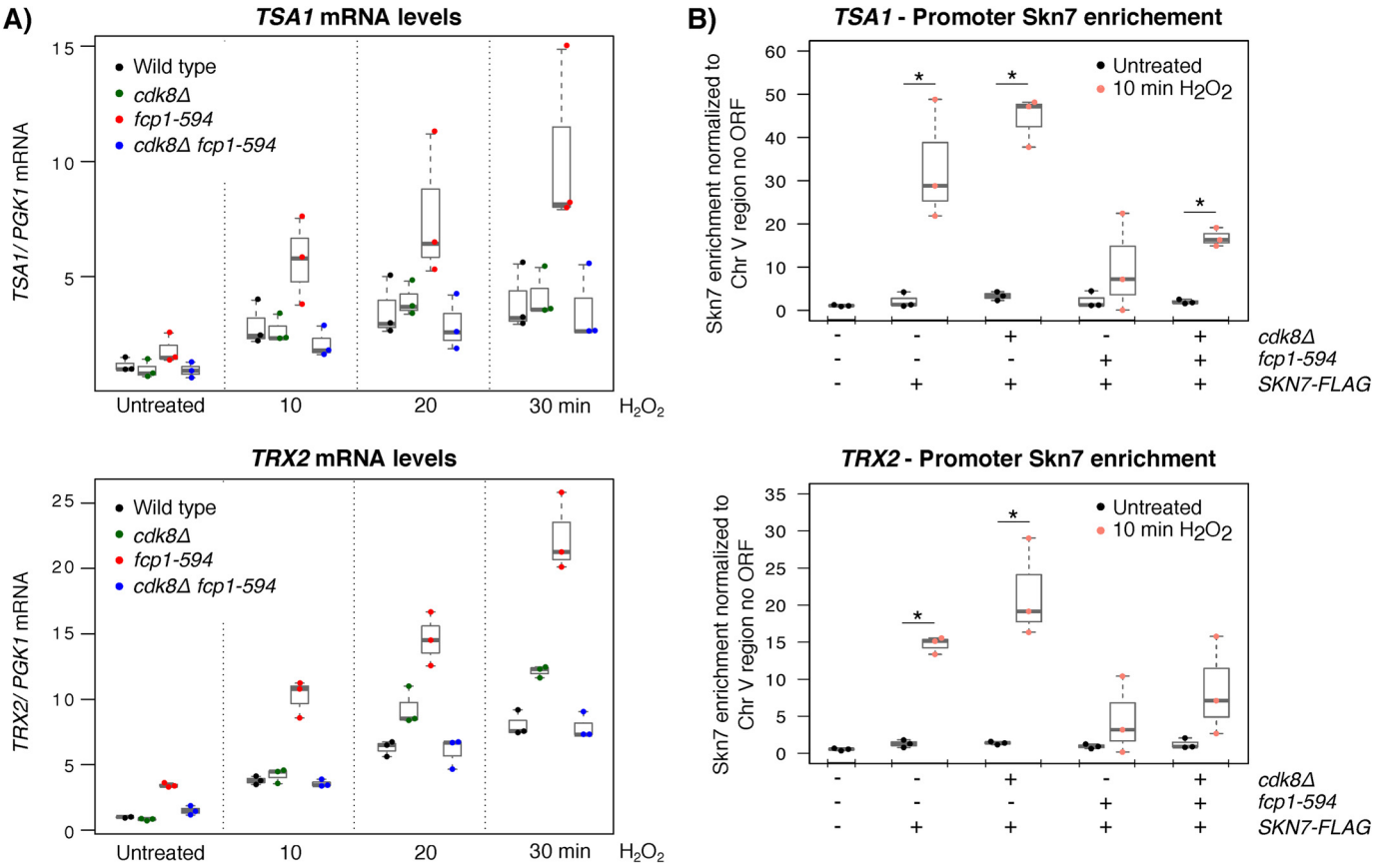

Figure 8. *FCP1* altered expression of *TSA1* and *TRX2* in a *CDK8*-dependent manner. *A*, RT-qPCR analysis of *TSA1* (*top*) and *TRX2* (*bottom*) mRNA levels with and without H_2O_2 treatment normalized to *PGK1* mRNA levels. The elevated *TRX2* and *TSA1* mRNA levels detected in the *fcp1-594* mutant were normalized by loss of *CDK8*. *B*, ChIP-qPCR analysis of Skn7 at the promoter of *TSA1* (*top*) and *TRX2* (*bottom*). Skn7 levels were normalized to an intergenic region of chromosome V (72). The *fcp1-594* mutant reduced Skn7 enrichment at the promoter of *TRX2* and *TSA1* upon induction. *, $p < 0.05$ using a two-tailed Student's *t* test. RT-qPCR and ChIP-qPCR results are shown as *box plots* displaying the median and interquartile range, with *whiskers* denoting 1.5 times the interquartile range.

genes compared with the promoters. For Skn7, a significant increase was also observed in the *cdk8*Δ mutant upon exposure to H_2O_2, an effect that tended to be higher compared with WT and was consistent with the observed stabilizing effect of the *cdk8*Δ mutant on Skn7. Most unexpected was the effect of the *fcp1-594* mutant, which despite robustly increasing *TRX2* and *TSA1* mRNA levels in a *SKN7*-dependent manner, showed no significant increase in Skn7 occupancy when comparing basal and inducing conditions. Loss of *CDK8* in the *fcp1-594* mutant background had limited effects on Skn7 occupancy at both the *TSA1* and *TRX2* promoters. Here, Skn7 occupancy remained low upon exposure to H_2O_2 compared with WT. However, we note that at the *TSA1* locus, loss of *CDK8* in the *fcp1-594* mutant background led to a significant difference between the uninduced and induced conditions.

The low Skn7 occupancy at the *TSA1* and *TRX2* promoter that we observed in the *fcp1-594* mutant prompted us to examine whether the gene expression alterations were linked to defects in transcription, which have been reported to increase the mRNA levels of stress-responsive genes through a combination of transcriptional and posttranscriptional effects (55). Here, we showed that inhibiting transcription by the addition of 100 μg/ml 1,10-phenanthroline increased *TSA1* and *TRX2* mRNA levels in the WT strain to levels similar to the untreated *fcp1-594* mutant (Fig. S6). Thus, defects in transcription in the *fcp1-594* mutant may in part underpin the gene expression alterations observed in this mutant under basal conditions. Comparing the effect of inhibiting transcription on the *fcp1-594* and *cdk8*Δ single and double mutants revealed that *TSA1* mRNA levels decreased in the *fcp1-594* mutant, increased in the *cdk8*Δ mutant, and more closely resembled the WT in the *fcp1-594 cdk8*Δ double mutant. Different patterns were observed for *TRX2*, suggesting that the effect of *FCP1* and *CDK8* in regulating the balance of transcriptional and posttranscriptional events was gene-specific.

Discussion

This study describes an unexpected role for *FCP1* and *CDK8* in the regulation of Skn7 and the expression of its target genes. We show that the genetic relationship between *FCP1* and *CDK8* upon exposure to oxidant depended on *SKN7* and that these factors modulated Skn7 protein levels, stability, and expression of target genes. Paradoxically, whereas the *fcp1-594* mutant increased expression of Skn7-dependent oxidative stress-induced genes, it decreased Skn7 promoter occupancy; the former was overcome by loss of *CDK8* likely through the stabilization of Skn7. As such, by probing the genes most sensitive to altered Fcp1 activity, our findings underscored a novel connection to *CDK8* in the regulation of Skn7 and the expression of its target loci.

Most defects of Skn7 biology observed in the *fcp1-594* mutant were normalized by loss of *CDK8*, revealing a shared function in the regulation of Skn7 and expanding well-known activities in the regulation of TFs and the transcriptional response to environmental stress (30, 31, 46, 56). Here, we observed that loss of *CDK8* normalized the growth defects of both the *fcp1-594* and *skn7*Δ mutants across a range of stress conditions, an effect that may be the result of the reported activation of stress-responsive genes upon loss of *CDK8* under basal conditions (57). Our findings also complemented previous work implicating *CDK8* in the biology of Skn7 as well as the oxidative stress response (48, 58–60). For instance, it has been shown that loss of *CDK8* can normalize the increased mRNA levels of *OCH1*, a Skn7-dependent osmotic stress-response gene, observed in a *not4*Δ mutant (which encodes a ubiquitin ligase subunit of the Ccr4-Not complex) (48). However, we note that whereas loss of *NOT4* increased Skn7 occupancy at the *OCH1* gene promoter (48), we observed that the *fcp1-594* mutant decreased Skn7 occupancy at the *TRX2* and *TSA1* promoters, suggesting that loss of *CDK8* may suppress Skn7-associated phenotypes in the *not4*Δ and *fcp1-594* mutant through distinct functional pathways. Cdk8 has also been implicated in the oxidative stress response by priming the degradation of Med13/Srb9, a Mediator kinase domain subunit (58). In fact, many Mediator subunits, including components of the kinase module (*e.g.* Med13 and CycC) have been implicated in the oxidative stress response and shown to be degraded upon oxidant exposure (58–60). Given that Cdk8 stability does not seem to be altered by exposure to oxidant, we hypothesize that the role described here may underscore a Mediator-independent activity for Cdk8.

Here, we report a role for *CDK8* in influencing Skn7 phosphorylation, protein levels, promoter occupancy, and expression of oxidative stress–induced genes, findings that are remarkably similar to *CDK8*'s effect on its reported direct TF substrates (30, 31, 46, 56, 61). Despite the similarities, our kinase assays did not support a direct kinase–substrate relationship between Cdk8 and Skn7, suggesting that either our kinase assays were missing important factors required for Skn7 phosphorylation or that the effects may be through indirect mechanisms. Consistent with the former, we note that Skn7 phosphorylation is complex, requiring Sln1 for phosphorylation by Ypd1 *in vitro* (47) and Yap1 for phosphorylation upon oxidative stress *in vivo* (62). Although some questions remain, Skn7 phosphorylation clearly is important for its activity as a transcriptional activator (62). At osmotic stress genes, phosphorylation of Asp-427 is required for their activation (45). During oxidative stress, Asp-427 phosphorylation is dispensable (52); although there is evidence that a number of Skn7 residues are phosphorylated under these conditions (62), their exact identity and responsible kinases remain unknown. Intriguingly, here we linked Skn7 phosphorylation and function in the oxidative stress response to Cdk8, a kinase that can bind Skn7 (48), and Fcp1, a protein phosphatase. However, their effects on Skn7 biology were not easily explained by direct phosphorylation and dephosphorylation by these factors. Therefore, it is formally possible that the effects of *FCP1* and *CDK8* on Skn7 function may be independent of its phosphorylation state. However, given that many sites on Skn7 have been suggested to undergo phosphorylation, it is also possible that the effect of *FCP1* and *CDK8* on Skn7 phosphorylation differ in a manner not readily detected by bulk shifts in migration patterns but that nonetheless result in functional differences to Skn7.

FCP1 has been previously implicated in the response to other environmental stressors. In fly-derived cell lines, *FCP1* knockdown leads to decreased expression and RNAPII association at heat shock genes (63), effects that contrasted the increased mRNA levels and RNAPII occupancy at oxidative stress response genes observed in yeast for the *fcp1-594* mutant. Although potentially indicative of species-specific activities, our yeast growth assays supported a distinct role for Fcp1 in the oxidative and heat shock response, showing that the sensitivity of the *fcp1-594* mutant to oxidative stress but not heat shock was suppressed by loss of *CDK8*. Altogether, here we show a role for Fcp1 in the transcriptional response to other environmental stressors while also revealing an ability to function as a transcriptional inhibitor, a particularly unexpected finding, given its well-established roles in facilitating transcription (6, 10).

Experimental procedures

Yeast strains

All yeast strains are listed in Table 1. They were primarily generated in the W303 background, with the exception of strains used for microarray expression profiling and E-MAP analysis, which were derived from a BY4742 background, the standard genotype for those assays. Complete or partial gene deletions and the integration of the 3XFLAG or HA tags were done using the one-step gene replacement method to integrate PCR-amplified segments (64). All double and triple mutant strains were generated via mating and tetrad dissection. All plasmids used are listed in Table 2.

Growth assays

Overnight cultures grown in YPD were diluted to 0.5 OD_{600}, 10-fold serially diluted, and spotted onto YPD plates with or without the indicated amount of HU (Sigma), MMS (Sigma), formamide (Sigma), hydrogen peroxide (H_2O_2) (Sigma), or sodium chloride (NaCl) (Bioshop). Plates were incubated at the indicated temperatures for 3–5 days.

Microarray experiments

Microarray expression profiling was performed in duplicate as described previously (65, 66). Cultures were grown in a 24-well plate incubator/reader to mid-log phase, with spiked-in RNA controls to monitor global changes in mRNA levels. Because no global changes in mRNA levels were detected, expression values were normalized to total mRNA levels. -Fold changes were determined by comparing mutant with WT profiles, with differentially expressed genes having a p value < 0.01 and absolute -fold change > 1.7 (67).

Data analysis

TF enrichment was done using the Yeast Promoter Atlas database and a hypergeometric test with Bonferroni correction

Table 1
Strains used in this study

Strain	Genotype	Background	Source
1810	*Mata fcp1–594-flag::nat his3Δ1 leu2Δ0 ura3Δ0*	BY4742	This study; gene expression
1811	*Mata fcp1–609-flag::nat his3Δ1 leu2Δ0 ura3Δ0*	BY4742	This study; gene expression
1812	*Mata fcp1–666-flag::nat his3Δ1 leu2Δ0 ura3Δ0*	BY4742	This study; gene expression
1813	*Mata fcp1–713-flag::nat his3Δ1 leu2Δ0 ura3Δ0*	BY4742	This study; gene expression
1814	*Mata FCP1-WT-flag::nat his3Δ1 leu2Δ0 ura3Δ0*	BY4742	This study; gene expression
1815	*Matα fcp1–594-flag::nat his3Δ 1 leu2Δ 0 LYS2+ met15Δ0 ura3Δ0 Δcan1::MATaPr-HIS3 Δlyp1::MATα Pr-LEU2*	BY4742	This study; E-MAP
1816	*Matα fcp1–609-flag::nat his3Δ 1 leu2Δ 0 LYS2+ met15Δ0 ura3Δ0 Δcan1::MATaPr-HIS3 Δlyp1::MATα Pr-LEU2*	BY4742	This study; E-MAP
1817	*Matα fcp1–666-flag::nat his3Δ 1 leu2Δ 0 LYS2+ met15Δ0 ura3Δ0 Δcan1::MATaPr-HIS3 Δlyp1::MATα Pr-LEU2*	BY4742	This study; E-MAP
1818	*Matα fcp1–713-flag::nat his3Δ 1 leu2Δ 0 LYS2+ met15Δ0 ura3Δ0Δcan1::MATaPr-HIS3 Δlyp1::MATα Pr-LEU2*	BY4742	This study; E-MAP
1819	*Matα FCP1-WT-flag::nat his3Δ 1 leu2Δ 0 LYS2+ met15Δ 0 ura3Δ 0 Δcan1::MATaPr-HIS3 Δlyp1::MATα Pr-LEU2*	BY4742	This study; E-MAP
1820	*Matα fcp1-594-flag::nat ade2-1 can1-100 his3-11 leu2-3, 112 trp 1-1 ura3-1 LYS2*	W303	This study
1821	*Matα fcp1-609-flag::nat ade2-1 can1-100 his3-11 leu2-3, 112 trp 1-1 ura3-1 LYS2*	W303	This study
1822	*Matα fcp1-666-flag::nat ade2-1 can1-100 his3-11 leu2-3, 112 trp 1-1 ura3-1 LYS2*	W303	This study
1823	*Matα fcp1-713-flag::nat ade2-1 can1-100 his3-11 leu2-3, 112 trp 1-1 ura3-1 LYS2*	W303	This study
1824	*Matα FCP1-flag::nat ade2-1 can1-100 his3-11 leu2-3, 112 trp 1-1 ura3-1 LYS2*	W303	This study
1825	*Matα Skn7-HA::kan ade2-1 can1-100 his3-11 leu2-3, 112 trp 1-1 ura3-1 LYS2*	W303	This study
1826	*Matα Skn7-HA::kan cdk8::his ade2-1 can1-100 his3-11 leu2-3, 112 trp 1-1 ura3-1 LYS2*	W303	This study
1827	*Matα Skn7-HA::kan fcp1-594-flag::nat ade2-1 can1-100 his3-11 leu2-3, 112 trp 1-1 ura3-1 LYS2*	W303	This study
1828	*Matα Skn7-HA::kan cdk8::his fcp1-594-flag::nat ade2-1 can1-100 his3-11 leu2-3, 112 trp 1-1 ura3-1 LYS2*	W303	This study
1829	*Matα Sok2-HA::kan ade2-1 can1-100 his3-11 leu2-3, 112 trp 1-1 ura3-1 LYS2*	W303	This study
1830	*Matα Sok2-HA::kan cdk8::his ade2-1 can1-100 his3-11 leu2-3, 112 trp 1-1 ura3-1 LYS2*	W303	This study
1831	*Matα Sok2-HA::kan fcp1-594-flag::nat ade2-1 can1-100 his3-11 leu2-3, 112 trp 1-1 ura3-1 LYS2*	W303	This study
1832	*Matα Sok2-HA::kan cdk8::his fcp1-594-flag::nat ade2-1 can1-100 his3-11 leu2-3, 112 trp 1-1 ura3-1 LYS2*	W303	This study
1833	*Matα Cad1-flag::kan ade2-1 can1-100 his3-11 leu2-3, 112 trp 1-1 ura3-1 LYS2*	W303	This study
1834	*Matα Cad1-flag::kan fcp1-594-HA::hygro ade2-1 can1-100 his3-11 leu2-3, 112 trp 1-1 ura3-1 LYS2*	W303	This study
1835	*Matα Mcm1-flag::kan ade2-1 can1-100 his3-11 leu2-3, 112 trp 1-1 ura3-1 LYS2*	W303	This study
1836	*Matα Mcm1-flag::kan fcp1-594-HA::hygro ade2-1 can1-100 his3-11 leu2-3, 112 trp 1-1 ura3-1 LYS2*	W303	This study
1837	*Matα Yap1-HA::kan ade2-1 can1-100 his3-11 leu2-3, 112 trp 1-1 ura3-1 LYS2*	W303	This study
1907	*Matα Yap1-HA::kan cdk8::his ade2-1 can1-100 his3-11 leu2-3, 112 trp 1-1 ura3-1 LYS2*	W303	This study
1838	*Matα Yap1-HA::kan fcp1-594-flag::nat ade2-1 can1-100 his3-11 leu2-3, 112 trp 1-1 ura3-1 LYS2*	W303	This study
1845	*Matα Yap1-HA::kan cdk8::his fcp1-594-flag::nat ade2-1 can1-100 his3-11 leu2-3, 112 trp 1-1 ura3-1 LYS2*	W303	This study
1839	*Matα skn7::Kan ade2-1 can1-100 his3-11 leu2-3, 112 trp 1-1 ura3-1 LYS2*	W303	This study
1840	*Matα skn7::Kan cdk8::his ade2-1 can1-100 his3-11 leu2-3, 112 trp 1-1 ura3-1 LYS2*	W303	This study
1841	*Matα skn7::Kan fcp1-594-flag::nat ade2-1 can1-100 his3-11 leu2-3, 112 trp 1-1 ura3-1 LYS2*	W303	This study
1842	*Matα skn7::Kan cdk8::his fcp1-594-flag::nat ade2-1 can1-100 his3-11 leu2-3, 112 trp 1-1 ura3-1 LYS2*	W303	This study
1901	*Matα sok2::Kan ade2-1 can1-100 his3-11 leu2-3, 112 trp 1-1 ura3-1 LYS2*	W303	This study
1902	*Matα sok2::Kan cdk8::his ade2-1 can1-100 his3-11 leu2-3, 112 trp 1-1 ura3-1 LYS2*	W303	This study
1903	*Matα sok2::Kan fcp1-594-flag::nat ade2-1 can1-100 his3-11 leu2-3, 112 trp 1-1 ura3-1 LYS2*	W303	This study
1904	*Matα sok2::Kan cdk8::his fcp1-594-flag::nat ade2-1 can1-100 his3-11 leu2-3, 112 trp 1-1 ura3-1 LYS2*	W303	This study
1905	*Matα cdk8::His ade2-1 can1-100 his3-11 leu2-3, 112 trp 1-1 ura3-1 LYS2*	W303	This study
1906	*Matα cdk8::His fcp1-594-flag::nat ade2-1 can1-100 his3-11 leu2-3, 112 trp 1-1 ura3-1 LYS2*	W303	This study
5	*Matα ade2-1 can1-100 his3-11 leu2-3, 112 trp 1-1 ura3-1 LYS2*	W303	
1908	*Matα Skn7-flag::kan ade2-1 can1-100 his3-11 leu2-3, 112 trp 1-1 ura3-1 LYS2*	W303	This study
1909	*Matα Skn7-flag::kan cdk8::his ade2-1 can1-100 his3-11 leu2-3, 112 trp 1-1 ura3-1 LYS2*	W303	This study
1910	*Matα Skn7-flag::kan fcp1-594-HA::hygro ade2-1 can1-100 his3-11 leu2-3, 112 trp 1-1 ura3-1 LYS2*	W303	This study
1911	*Matα Skn7-flag::kan cdk8::his fcp1-594-HA::hygro ade2-1 can1-100 his3-11 leu2-3, 112 trp 1-1 ura3-1 LYS2*	W303	This study
YCN44	*Mata ura3-52 cdk8::URA3*	Σ1278b	Ref. 74

Table 2
Plasmids used in this study

Plasmid	Details	Source
pIS484	*URA3 ARS-CEN TEF1* promoter–Σ1278b *CDK8*-3×FLAG–His_6	Ref. 31
pIS529	*URA3 ARS-CEN TEF1* promoter–Σ1278b *CDK8D290A*–3×FLAG–His_6	Ref. 31
pMK660	*TRP1 ARS-CEN CDK8*	This study
pMK661	*TRP1 ARS-CEN cdk8D290A*	This study

(adjusted p value of 0.05) (29). The gene expression profile for the *cdk8*Δ mutant was reported previously (33). TFs with a score greater than 6.4 in the YeastKID database were categorized as phosphorylated, and a hypergeometric test was used to test for significance ($p = 0.03355$) (35). Complete gene expression profiles can be found in GSE128936.

Protein extraction and protein blotting

Overnight cultures were diluted to 0.3 OD_{600} and grown to 1.0 OD_{600}. Whole-cell extracts were prepared by glass bead lysis in the presence of TCA. Immunoblotting was done using anti-HA (Sigma), anti-FLAG (Sigma), or actin (ICN) antibodies. Immunoblots were scanned with the Odyssey IR imaging system (LI-COR).

RT-qPCR

Overnight cultures were diluted to 0.15 OD_{600} and grown to 0.5 OD_{600}. RNA was extracted and purified using the Qiagen RNeasy minikit. cDNA was generated using the Qiagen QuantiTect reverse transcription kit and analyzed using the PerfeCTa SYBR Green FastMix (VWR) and a Rotor-Gene 6000

Table 3
Primers used in this study

Primer name	Forward sequence	Reverse sequence	Source or reference
SKN7 RT-qPCR	GCGACGGTCTTTCAGCTATC	AAATCATCCCTCGTGAATGG	This study
SOK2 RT-qPCR	GGGTGTCTGGATACCGTTTG	ATAGGTACGCGGACTGATGG	This study
MCM1 RT-qPCR	CATCCTCGACCACAGCAAG	GGCAAAAGCCTGTTGGTG	This study
CAD1 RT-qPCR	CTTTATTCCCCAGCGTGCTT	GGAAGCACCGAAGCTAGAGA	This study
TUB1 RT-qPCR	TCTTGGTGGTGGTACTGGTT	TGGATTTCTTACCGTATTCAGCG	Ref. 75
TSA1 3′ and RT-qPCR	GGCTGACACCAACCACTCTT	TTGGAAGGCTTCAACCAATC	This study
TRX2 3′ and RT-qPCR	AGCTGAAGTTTCTTCCATGCCT	TTGATAGCAGCTGGGTTGGC	This study
PGK1 RT-qPCR	CAAGAGCTCTGCTGCTGGTA	AAAGCAACACCTGGCAATTC	This study
TSA1 promoter	TGGCAACAAACCAGGACATA	TGTGGTTGGTTGTGAGCAAT	This study
TRX2 promoter	CCATTCGGGGGATGAAAAG	TCGTAGACTCTCGTGTATGTGTG	This study
Chr V	GGCTGTCAGAATATGGGGCCGTAGTA	CACCCCGAAGCTGCTTTCACAATAC	Ref. 72
RIB5 RT-qPCR	CGCAAGGTGGAGCCTTCTAT	TGCTTCTCAATAATCTTCCCAGT	This study
SNR19 RT-qPCR	ACTTTTCTCTAGCGTGCCAT	CTTCAAACTACAATCCCGACCA	This study

(Qiagen). All strains were grown in YPD, except for strains carrying pRS314-based vectors, which were grown in −TRP medium. 0.2 mM H_2O_2 or 100 μg/ml 1,10-phenanthroline were used to treat cells for the indicated amount of time. *TUB1*, *PKG1*, *RIB5*, and *SNR19* were used as control genes as indicated. The choice of control gene depended on the stability of the gene in the condition tested. *PKG1* was used for experiments involving oxidative stress, and a composite of *RIB5* (68) and *SNR19* (69) was used for experiments involving transcriptional inhibition. mRNA levels were quantified from three independent biological replicates. All primer sequences used are listed in Table 3.

E-MAP

E-MAP screens were performed as described previously (36). Briefly, *FCP1* mutants were crossed, using a Singer robot, to a library of 1536 mutants, including full gene deletions or DAmP (decrease abundance by mRNA perturbation) alleles. Mating, diploid selection, sporulation, haploid selection, and double mutant selection were done by replicate plating on selective media, as described previously. All strains were screened in triplicate, and normalization was performed as described previously (36). *S* scores ≥2 and ≤−2.5 were considered significant.

Protein stability assay

Overnight cultures were diluted to 0.3 OD_{600} and grown to 1.0 OD_{600}. 10 OD_{600} units were collected prior to the addition of 100 μg/ml cycloheximide (Sigma). Following protein shutdown, 10 OD_{600} units were collected at the indicated times. All proteins were extracted using TCA as described above. Due to the differences in starting protein levels in the *FCP1* mutant, protein loading was adjusted as indicated in each figure. Signal intensities from each lane were used to calculate percentage protein levels relative to the untreated control.

Immunoprecipitation (IP) and phosphatase treatment

The phosphatase treatment protocol was adapted from Flott and Rouse (70). Overnight cultures were diluted to 0.3 OD_{600} and grown to 1.0 OD_{600}. Samples were mechanically lysed in TAP-IP buffer (50 mM Tris (pH 7.8), 150 mM NaCl, 1.5 mM MgAc, 10% glycerol, 0.15% Nonidet P40, 1 mM DTT) with phosphatase inhibitors (10 mM $NaPP_i$, 5 mM EGTA, 5 mM EDTA, 0.1 mM Na_3VO_4, and 5 mM NaF) and Complete EDTA-free protease inhibitor mixture (Roche Applied Science). Lysates were split equally into three tubes containing 40 μl of HA beads (Sigma) and incubated for 1.5 h. Samples were washed twice with TAP-IP buffer with phosphatase and protease inhibitors and twice with TAP-IP buffer lacking phosphatase and protease inhibitors prior to resuspending in 1× NEBuffer for protein metallophosphatases (50 mM HEPES, 100 mM NaCl, 2 mM DTT, 0.01% Brij 35, 1 mM $MnCl_2$). 200 units of λ-phosphatase (New England BioLabs) and 100 mM EDTA was added as indicated and incubated for 60 min at 30 °C. Samples were washed twice using Tandem Affinity Purification (TAP)-IP buffer without phosphatase and protease inhibitors and resuspended in 2× SDS buffer prior to analysis by SDS-PAGE. Protein loading was adjusted as indicated in an effort to ensure that the differences in protein migration were not influenced by changes in the amount of protein in each sample.

Recombinant protein expression

An N-terminally 6×HIS-tagged *SKN7* was cloned into a pET28a derivative and expressed from *Escherichia coli* BL21 (DE3)-RIL cells. Cells were induced at 0.6 OD_{600} for 4 h at 37 °C using 1.0 mM isopropyl 1-thio-β-D-galactopyranoside, harvested by centrifugation, and lysed in buffer containing 25 mM Tris-Cl (pH 7.5), 0.5 M NaCl, 30 mM imidazole, and 1 mg/ml lysozyme. Skn7 protein was purified by passing the supernatant over a HisTrap FF (5 ml) column (GE Healthcare) and eluted using 0.5 M imidazole.

In vitro kinase assays

The *in vitro* kinase assay protocol was adapted from Hirst *et al.* (56). Strains from a Σ1278b background, expressing either WT or kinase-impaired FLAG-tagged *CDK8* (D290A), were grown to 1.0 OD_{600}. Cells were collected and mechanically lysed in kinase lysis buffer (KLB) (50 mM Tris, 200 mM NaCl, 5 mM EDTA, 0.1% Nonidet P40, and protease inhibitors). Cdk8 was immunoprecipitated by incubating cell lysates with anti-FLAG M2 beads for 60 min, followed by two washes with KLB and two washes with kinase buffer (10 mM $MgCl_2$, 50 mM Tris (pH 7.5), 1 mM DTT, and protease inhibitors). Kinase reactions were performed for 20 min at 30 °C in kinase buffer, with 3.33 pmol of [γ-^{32}P]ATP (PerkinElmer Life Sciences) and 1 μg of the indicated substrate. Reactions were run on a 10% SDS-polyacrylamide gel and exposed on Kodak Biomax film.

ChIP

Overnight cultures were diluted to 0.15 OD_{600}, grown to 0.5 OD_{600}, and cross-linked or induced using 0.2 mM H_2O_2 for 10 min prior to cross-linking with 1% formaldehyde for 20 min. Chromatin was prepared as described previously (71). Anti-FLAG antibody (4.2 μl) (Sigma) or anti-Rpb3 antibody (7 μl) (Neoclone) was coupled to 60 μl of Protein A Dynabeads (Invitrogen) overnight. Following cross-linking reversal and DNA purification, both the immunoprecipitated and input DNA were analyzed by qPCR using a Rotor-Gene 6000 and PerfeCTa SYBR Green FastMix (Quanta Biosciences). All samples were analyzed from three independent biological replicates and normalized to an intragenic region of Chromosome V (72). Primers used are listed in Table 3.

ChIP-on-chip analysis

Cdk8 ChIP-on-chip profiles were reported previously (35). Average scores were obtained by averaging all probes mapping to 500 bp upstream of the ORF. TF target gene pairs were obtained from the YEASTRACT database using the DNA binding and expression evidence category (73). Genes that are regulated by more than one TF were included in the respective box plots.

Author contributions—M. J. A., K. D., and M. S. K. conceptualization; M. J. A. data curation; M. J. A., G. L. N., and J. J. B. formal analysis; M. J. A., F. C. H., N. J. K., I. S., and M. S. K. supervision; M. J. A. and M. S. K. funding acquisition; M. J. A., K. D., M. S., N. H., J. J. B., F. C. H., N. J. K., and I. S. investigation; M. J. A. visualization; M. J. A., K. D., F. C. H., N. J. K., and I. S. methodology; M. J. A. and K. D. writing-original draft; M. J. A., G. L. N., F. C. H., N. J. K., I. S., and M. S. K. writing-review and editing.

Acknowledgments—We thank Dr. Emanuel Rosonina for insightful discussions, Dr. Alexandre Lussier for critical reading of the manuscript, Alyssa Kirlin for assistance with the purification of Skn7 and critical reading of the manuscript, Marian Groot Koerkamp for help with the microarray data submission, and Konstantin Mestnikov for help with the 1,10-phenanthroline exposure experiment.

References

1. Allison, L. A., and Ingles, C. J. (1989) Mutations in RNA polymerase II enhance or suppress mutations in GAL4. *Proc. Natl. Acad. Sci. U.S.A.* **86,** 2794–2798 CrossRef Medline
2. Nonet, M., Sweetser, D., and Young, R. A. (1987) Functional redundancy and structural polymorphism in the large subunit of RNA polymerase II. *Cell* **50,** 909–915 CrossRef Medline
3. Corden, J. L., Cadena, D. L., Ahearn, J. M., Jr., and Dahmus, M. E. (1985) A unique structure at the carboxyl terminus of the largest subunit of eukaryotic RNA polymerase II. *Proc. Natl. Acad. Sci. U.S.A.* **82,** 7934–7938 CrossRef Medline
4. Harlen, K. M., and Churchman, L. S. (2017) The code and beyond: transcription regulation by the RNA polymerase II carboxy-terminal domain. *Nat. Rev. Mol. Cell Biol.* **18,** 263–273 CrossRef Medline
5. Zaborowska, J., Egloff, S., and Murphy, S. (2016) The pol II CTD: new twists in the tail. *Nat. Struct. Mol. Biol.* **23,** 771–777 CrossRef Medline
6. Kobor, M. S., Archambault, J., Lester, W., Holstege, F. C. P., Gileadi, O., Jansma, D. B., Jennings, E. G., Kouyoumdjian, F., Davidson, A. R., Young, R. A., and Greenblatt, J. (1999) An unusual eukaryotic protein phosphatase required for transcription by RNA polymerase II and CTD dephosphorylation in S. cerevisiae. *Mol. Cell* **4,** 55–62 CrossRef Medline
7. Kimura, M., Suzuki, H., and Ishihama, A. (2002) Formation of a carboxy-terminal domain phosphatase (Fcp1)/TFIIF/RNA polymerase II (pol II) complex in *Schizosaccharomyces pombe* involves direct interaction between Fcp1 and the Rpb4 subunit of pol II. *Mol. Cell Biol.* **22,** 1577–1588 CrossRef Medline
8. Archambault, J., Chambers, R. S., Kobor, M. S., Ho, Y., Cartier, M., Bolotin, D., Andrews, B., Kane, C. M., and Greenblatt, J. (1997) An essential component of a C-terminal domain phosphatase that interacts with transcription factor IIF in *Saccharomyces cerevisiae*. *Proc. Natl. Acad. Sci. U.S.A.* **94,** 14300–14305 CrossRef Medline
9. Ghosh, A., Shuman, S., and Lima, C. D. (2008) The structure of Fcp1, an essential RNA polymerase II CTD phosphatase. *Mol. Cell* **32,** 478–490 CrossRef Medline
10. Kobor, M. S., Simon, L. D., Omichinski, J., Zhong, G., Archambault, J., and Greenblatt, J. (2000) A motif Shared by TFIIF and TFIIB mediates their interaction with the RNA polymerase II carboxy-terminal domain phosphatase Fcp1p in *Saccharomyces cerevisiae*. *Mol. Cell Biol.* **20,** 7438–7449 CrossRef Medline
11. Yu, X., Chini, C. C., He, M., Mer, G., and Chen, J. (2003) The BRCT domain is a phospho-protein binding domain. *Science* **302,** 639–642 CrossRef Medline
12. Zhang, D. W., Mosley, A. L., Ramisetty, S. R., Rodríguez-Molina, J. B., Washburn, M. P., and Ansari, A. Z. (2012) Ssu72 phosphatase-dependent erasure of phospho-Ser7 marks on the RNA polymerase II C-terminal domain is essential for viability and transcription termination. *J. Biol. Chem.* **287,** 8541–8551 CrossRef Medline
13. Cho, E.-J., Kobor, M. S., Kim, M., Greenblatt, J., and Buratowski, S. (2001) Opposing effects of Ctk1 kinase and Fcp1 phosphatase at Ser 2 of the RNA polymerase II C-terminal domain. *Genes Dev.* **15,** 3319–3329 CrossRef Medline
14. Bataille, A. R., Jeronimo, C., Jacques, P.-É., Laramée, L., Fortin, M.-È., Forest, A., Bergeron, M., Hanes, S. D., and Robert, F. (2012) A Universal RNA Polymerase II CTD Cycle Is Orchestrated by Complex Interplays between Kinase, Phosphatase, and Isomerase Enzymes along Genes. *Molecular Cell* **45,** 158–170 CrossRef Medline
15. Hsin, J.-P., Xiang, K., and Manley, J. L. (2014) Function and control of RNA polymerase II C-terminal domain phosphorylation in vertebrate transcription and RNA processing. *Mol. Cell Biol.* **34,** 2488–2498 CrossRef Medline
16. Calvo, O., and Manley, J. L. (2005) The transcriptional coactivator PC4/Sub1 has multiple functions in RNA polymerase II transcription. *EMBO J.* **24,** 1009–1020 CrossRef Medline
17. Suh, M.-H., Ye, P., Zhang, M., Hausmann, S., Shuman, S., Gnatt, A. L., and Fu, J. (2005) Fcp1 directly recognizes the C-terminal domain (CTD) and interacts with a site on RNA polymerase II distinct from the CTD. *Proc. Natl. Acad. Sci. U.S.A.* **102,** 17314–17319 CrossRef Medline
18. Kops, O., Zhou, X. Z., and Lu, K. P. (2002) Pin1 modulates the dephosphorylation of the RNA polymerase II C-terminal domain by yeast Fcp1. *FEBS Lett.* **513,** 305–311 CrossRef Medline
19. Chambers, R. S., Wang, B. Q., Burton, Z. F., and Dahmus, M. E. (1995) The activity of COOH-terminal domain phosphatase is regulated by a docking site on RNA polymerase II and by the general transcription factors IIF and IIB. *J. Biol. Chem.* **270,** 14962–14969 CrossRef Medline
20. Garavís, M., González-Polo, N., Allepuz-Fuster, P., Louro, J. A., Fernández-Tornero, C., and Calvo, O. (2017) Sub1 contacts the RNA polymerase II stalk to modulate mRNA synthesis. *Nucleic Acids Res.* **45,** 2458–2471 CrossRef Medline
21. Zhang, B., Yang, G., Chen, Y., Zhao, Y., Gao, P., Liu, B., Wang, H., and Zheng, Z.-L. (2016) C-terminal domain (CTD) phosphatase links Rho GTPase signaling to Pol II CTD phosphorylation in *Arabidopsis* and yeast. *Proc. Natl. Acad. Sci. U.S.A.* **113,** E8197–E8206 CrossRef Medline
22. Schwer, B., Ghosh, A., Sanchez, A. M., Lima, C. D., and Shuman, S. (2015) Genetic and structural analysis of the essential fission yeast RNA polymerase II CTD phosphatase Fcp1. *RNA* **21,** 1135–1146 CrossRef Medline
23. Visconti, R., Palazzo, L., Della Monica, R., and Grieco, D. (2012) Fcp1-dependent dephosphorylation is required for M-phase-promoting factor inactivation at mitosis exit. *Nat. Commun.* **3,** 894 CrossRef Medline

24. Hégarat, N., Vesely, C., Vinod, P. K., Ocasio, C., Peter, N., Gannon, J., Oliver, A. W., Novák, B., and Hochegger, H. (2014) PP2A/B55 and Fcp1 regulate Greatwall and Ensa dephosphorylation during mitotic exit. *PLoS Genet.* **10,** e1004004 CrossRef Medline
25. Della Monica, R., Visconti, R., Cervone, N., Serpico, A. F., and Grieco, D. (2015) Fcp1 phosphatase controls Greatwall kinase to promote PP2A-B55 activation and mitotic progression. *eLife* **4,** e10399 CrossRef Medline
26. Bierhoff, H., Dundr, M., Michels, A. A., and Grummt, I. (2008) Phosphorylation by casein kinase 2 facilitates rRNA gene transcription by promoting dissociation of TIF-IA from elongating RNA polymerase I. *Mol. Cell Biol.* **28,** 4988–4998 CrossRef Medline
27. Fath, S., Kobor, M. S., Philippi, A., Greenblatt, J., and Tschochner, H. (2004) Dephosphorylation of RNA polymerase I by Fcp1p is required for efficient rRNA synthesis. *J. Biol. Chem.* **279,** 25251–25259 CrossRef Medline
28. Guo, Z., and Stiller, J. W. (2005) Comparative genomics and evolution of proteins associated with RNA polymerase II C-terminal domain. *Mol. Biol. Evol.* **22,** 2166–2178 CrossRef Medline
29. Chang, D. T.-H., Huang, C.-Y., Wu, C.-Y., and Wu, W.-S. (2011) YPA: an integrated repository of promoter features in *Saccharomyces cerevisiae*. *Nucleic Acids Res.* **39,** D647–D652 CrossRef Medline
30. Raithatha, S., Su, T.-C., Lourenco, P., Goto, S., and Sadowski, I. (2012) Cdk8 regulates stability of the transcription factor Phd1 to control pseudohyphal differentiation of *Saccharomyces cerevisiae*. *Mol. Cell Biol.* **32,** 664–674 CrossRef Medline
31. Nelson, C., Goto, S., Lund, K., Hung, W., and Sadowski, I. (2003) Srb10/Cdk8 regulates yeast filamentous growth by phosphorylating the transcription factor Ste12. *Nature* **421,** 187–190 CrossRef Medline
32. Byrne, K. P., and Wolfe, K. H. (2005) The Yeast Gene Order Browser: combining curated homology and syntenic context reveals gene fate in polyploid species. *Genome Res.* **15,** 1456–1461 CrossRef Medline
33. van de Peppel, J., Kettelarij, N., van Bakel, H., Kockelkorn, T. T. J. P., van Leenen, D., and Holstege, F. C. P. (2005) Mediator expression profiling epistasis reveals a signal transduction pathway with antagonistic submodules and highly specific downstream targets. *Mol. Cell* **19,** 511–522 CrossRef Medline
34. Aristizabal, M. J., Negri, G. L., Benschop, J. J., Holstege, F. C. P., Krogan, N. J., and Kobor, M. S. (2013) High-throughput genetic and gene expression analysis of the RNAPII-CTD reveals unexpected connections to SRB10/CDK8. *PLoS Genet.* **9,** e1003758 CrossRef Medline
35. Sharifpoor, S., Nguyen Ba, A. N., Young, J.-Y., van Dyk, D., Friesen, H., Douglas, A. C., Kurat, C. F., Chong, Y. T., Founk, K., Moses, A. M., and Andrews, B. J. (2011) A quantitative literature-curated gold standard for kinase-substrate pairs. *Genome Biol.* **12,** R39 CrossRef Medline
36. Collins, S. R., Roguev, A., and Krogan, N. J. (2010) Quantitative genetic interaction mapping using the E-MAP approach. *Methods Enzymol.* **470,** 205–231 CrossRef Medline
37. Hsu, P. L., Yang, F., Smith-Kinnaman, W., Yang, W., Song, J.-E., Mosley, A. L., and Varani, G. (2014) Rtr1 is a dual specificity phosphatase that dephosphorylates Tyr1 and Ser5 on the RNA polymerase II CTD. *J. Mol. Biol.* **426,** 2970–2981 CrossRef Medline
38. Mosley, A. L., Pattenden, S. G., Carey, M., Venkatesh, S., Gilmore, J. M., Florens, L., Workman, J. L., and Washburn, M. P. (2009) Rtr1 is a CTD phosphatase that regulates RNA polymerase II during the transition from serine 5 to serine 2 phosphorylation. *Mol. Cell* **34,** 168–178 CrossRef Medline
39. Wu, X., Wilcox, C. B., Devasahayam, G., Hackett, R. L., Arévalo-Rodríguez, M., Cardenas, M. E., Heitman, J., and Hanes, S. D. (2000) The Ess1 prolyl isomerase is linked to chromatin remodeling complexes and the general transcription machinery. *EMBO J.* **19,** 3727–3738 CrossRef Medline
40. Lee, J. M., and Greenleaf, A. L. (1991) CTD kinase large subunit is encoded by CTK1, a gene required for normal growth of *Saccharomyces cerevisiae*. *Gene Expr.* **1,** 149–167 Medline
41. Ng, H. H., Robert, F., Young, R. A., and Struhl, K. (2003) Targeted recruitment of Set1 histone methylase by elongating Pol II provides a localized mark and memory of recent transcriptional activity. *Mol. Cell* **11,** 709–719 CrossRef Medline
42. Mulford, K. E., and Fassler, J. S. (2011) Association of the Skn7 and Yap1 transcription factors in the *Saccharomyces cerevisiae* oxidative stress response. *Eukaryotic Cell* **10,** 761–769 CrossRef Medline
43. Krems, B., Charizanis, C., and Entian, K.-D. (1996) The response regulator-like protein Pos9/Skn7 ofSaccharomyces cerevisiae is involved in oxidative stress resistance. *Curr. Genet.* **29,** 327–334 CrossRef Medline
44. Raitt, D. C., Johnson, A. L., Erkine, A. M., Makino, K., Morgan, B., Gross, D. S., and Johnston, L. H. (2000) The Skn7 response regulator of *Saccharomyces cerevisiae* interacts with Hsf1 *in vivo* and is required for the induction of heat shock genes by oxidative stress. *Mol. Biol. Cell* **11,** 2335–2347 CrossRef Medline
45. Ketela, T., Brown, J. L., Stewart, R. C., and Bussey, H. (1998) Yeast Skn7p activity is modulated by the Sln1p-Ypd1p osmosensor and contributes to regulation of the HOG pathway. *Mol. Gen. Genet.* **259,** 372–378 CrossRef Medline
46. Chi, Y., Huddleston, M. J., Zhang, X., Young, R. A., Annan, R. S., Carr, S. A., and Deshaies, R. J. (2001) Negative regulation of Gcn4 and Msn2 transcription factors by Srb10 cyclin-dependent kinase. *Genes Dev.* **15,** 1078–1092 CrossRef Medline
47. Li, S., Ault, A., Malone, C. L., Raitt, D., Dean, S., Johnston, L. H., Deschenes, R. J., and Fassler, J. S. (1998) The yeast histidine protein kinase, Sln1p, mediates phosphotransfer to two response regulators, Ssk1p and Skn7p. *EMBO J.* **17,** 6952–6962 CrossRef Medline
48. Lenssen, E., Azzouz, N., Michel, A., Landrieux, E., and Collart, M. A. (2007) The Ccr4-Not complex regulates Skn7 through Srb10 kinase. *Eukaryot. Cell* **6,** 2251–2259 CrossRef Medline
49. Hengartner, C. J., Myer, V. E., Liao, S.-M., Wilson, C. J., Koh, S. S., and Young, R. A. (1998) Temporal regulation of RNA polymerase II by Srb10 and Kin28 cyclin-dependent kinases. *Mol. Cell* **2,** 43–53 CrossRef Medline
50. Liu, Y., Kung, C., Fishburn, J., Ansari, A. Z., Shokat, K. M., and Hahn, S. (2004) Two cyclin-dependent kinases promote RNA polymerase II transcription and formation of the scaffold complex. *Mol. Cell Biol.* **24,** 1721–1735 CrossRef Medline
51. Liao, S.-M., Zhang, J., Jeffery, D. A., Koleske, A. J., Thompson, C. M., Chao, D. M., Viljoen, M., van Vuuren, H. J. J., Young, R. A. (1995) A kinase–cyclin pair in the RNA polymerase II holoenzyme. *Nature* **374,** 193–196 CrossRef Medline
52. Morgan, B. A., Banks, G. R., Toone, W. M., Raitt, D., Kuge, S., and Johnston, L. H. (1997) The Skn7 response regulator controls gene expression in the oxidative stress response of the budding yeast *Saccharomyces cerevisiae*. *EMBO J.* **16,** 1035–1044 CrossRef Medline
53. Lee, J., Godon, C., Lagniel, G., Spector, D., Garin, J., Labarre, J., and Toledano, M. B. (1999) Yap1 and Skn7 control two specialized oxidative stress response regulons in yeast. *J. Biol. Chem.* **274,** 16040–16046 CrossRef Medline
54. He, X.-J., and Fassler, J. S. (2005) Identification of novel Yap1p and Skn7p binding sites involved in the oxidative stress response of *Saccharomyces cerevisiae*. *Mol. Microbiol.* **58,** 1454–1467 CrossRef Medline
55. Grigull, J., Mnaimneh, S., Pootoolal, J., Robinson, M. D., and Hughes, T. R. (2004) Genome-wide analysis of mRNA stability using transcription inhibitors and microarrays reveals posttranscriptional control of ribosome biogenesis factors. *Mol. Cell Biol.* **24,** 5534–5547 CrossRef Medline
56. Hirst, M., Kobor, M. S., Kuriakose, N., Greenblatt, J., and Sadowski, I. (1999) GAL4 is regulated by the RNA polymerase II holoenzyme–associated cyclin-dependent protein kinase SRB10/CDK8. *Mol. Cell* **3,** 673–678 CrossRef Medline
57. Holstege, F. C. P., Jennings, E. G., Wyrick, J. J., Lee, T. I., Hengartner, C. J., Green, M. R., Golub, T. R., Lander, E. S., and Young, R. A. (1998) Dissecting the regulatory circuitry of a eukaryotic genome. *Cell* **95,** 717–728 CrossRef Medline
58. Willis, S. D., Stieg, D. C., Ong, K. L., Shah, R., Strich, A. K., Grose, J. H., and Cooper, K. F. (2018) Snf1 cooperates with the CWI MAPK pathway to mediate the degradation of Med13 following oxidative stress. *Microbial Cell* **5,** 357–370 CrossRef Medline
59. Cooper, K. F., Scarnati, M. S., Krasley, E., Mallory, M. J., Jin, C., Law, M. J., and Strich, R. (2012) Oxidative-stress-induced nuclear to cytoplasmic relocalization is required for Not4-dependent cyclin C destruction. *J. Cell Sci.* **125,** 1015–1026 CrossRef Medline

60. Krasley, E., Cooper, K. F., Mallory, M. J., Dunbrack, R., and Strich, R. (2006) Regulation of the oxidative stress response through Slt2p-dependent destruction of cyclin C in *Saccharomyces cerevisiae*. *Genetics* **172,** 1477–1486 CrossRef Medline
61. Rosonina, E., Duncan, S. M., and Manley, J. L. (2012) Sumoylation of transcription factor Gcn4 facilitates its Srb10-mediated clearance from promoters in yeast. *Genes Dev.* **26,** 350–355 CrossRef Medline
62. He, X.-J., Mulford, K. E., and Fassler, J. S. (2009) Oxidative stress function of the *Saccharomyces cerevisiae* Skn7 receiver domain. *Eukaryot. Cell* **8,** 768–778 CrossRef Medline
63. Fuda, N. J., Buckley, M. S., Wei, W., Core, L. J., Waters, C. T., Reinberg, D., and Lis, J. T. (2012) Fcp1 dephosphorylation of the RNA polymerase II C-terminal domain is required for efficient transcription of heat shock genes. *Mol. Cell Biol.* **32,** 3428–3437 CrossRef Medline
64. Longtine, M. S., McKenzie, A., 3rd, Demarini, D. J., Shah, N. G., Wach, A., Brachat, A., Philippsen, P., and Pringle, J. R. (1998) Additional modules for versatile and economical PCR-based gene deletion and modification in *Saccharomyces cerevisiae*. *Yeast* **14,** 953–961 CrossRef Medline
65. Lenstra, T. L., Benschop, J. J., Kim, T., Schulze, J. M., Brabers, N. A. C. H., Margaritis, T., van de Pasch, L. A. L., van Heesch, S. A. A. C., Brok, M. O., Groot Koerkamp, M. J. A., Ko, C. W., van Leenen, D., Sameith, K., van Hooff, S. R., Lijnzaad, P., *et al.* (2011) The specificity and topology of chromatin interaction pathways in yeast. *Mol. Cell* **42,** 536–549 CrossRef Medline
66. van Wageningen, S., Kemmeren, P., Lijnzaad, P., Margaritis, T., Benschop, J. J., de Castro, I. J., van Leenen, D., Groot Koerkamp, M. J. A., Ko, C. W., Miles, A. J., Brabers, N., Brok, M. O., Lenstra, T. L., Fiedler, D., Fokkens, L., *et al.* (2010) Functional overlap and regulatory links shape genetic interactions between signaling pathways. *Cell* **143,** 991–1004 CrossRef Medline
67. Kemmeren, P., Sameith, K., van de Pasch, L. A. L., Benschop, J. J., Lenstra, T. L., Margaritis, T., O'Duibhir, E., Apweiler, E., van Wageningen, S., Ko, C. W., van Heesch, S., Kashani, M. M., Ampatziadis-Michailidis, G., Brok, M. O., Brabers, N. A. C. H., *et al.* (2014) Large-scale genetic perturbations reveal regulatory networks and an abundance of gene-specific repressors. *Cell* **157,** 740–752 CrossRef Medline
68. Molin, C., Jauhiainen, A., Warringer, J., Nerman, O., and Sunnerhagen, P. (2009) mRNA stability changes precede changes in steady-state mRNA amounts during hyperosmotic stress. *RNA* **15,** 600–614 CrossRef Medline
69. Molina-Navarro, M. M., Castells-Roca, L., Bellí, G., García-Martínez, J., Marín-Navarro, J., Moreno, J., Pérez-Ortín, J. E., and Herrero, E. (2008) Comprehensive transcriptional analysis of the oxidative response in yeast. *J. Biol. Chem.* **283,** 17908–17918 CrossRef Medline
70. Flott, S., and Rouse, J. (2005) Slx4 becomes phosphorylated after DNA damage in a Mec1/Tel1-dependent manner and is required for repair of DNA alkylation damage. *Biochem. J.* **391,** 325–333 CrossRef Medline
71. Schulze, J. M., Jackson, J., Nakanishi, S., Gardner, J. M., Hentrich, T., Haug, J., Johnston, M., Jaspersen, S. L., Kobor, M. S., and Shilatifard, A. (2009) Linking cell cycle to histone modifications: SBF and H2B monoubiquitination machinery and cell-cycle regulation of H3K79 dimethylation. *Mol. Cell* **35,** 626–641 CrossRef Medline
72. Keogh, M.-C., and Buratowski, S. (2004) Using chromatin immunoprecipitation to map cotranscriptional mRNA processing in *Saccharomyces cerevisiae*. *Methods Mol. Biol.* **257,** 1–16 CrossRef Medline
73. Teixeira, M. C., Monteiro, P. T., Palma, M., Costa, C., Godinho, C. P., Pais, P., Cavalheiro, M., Antunes, M., Lemos, A., Pedreira, T., and Sá-Correia, I. (2018) YEASTRACT: an upgraded database for the analysis of transcription regulatory networks in *Saccharomyces cerevisiae*. *Nucleic Acids Res.* **46,** D348–D353 CrossRef Medline
74. Pan, X., and Heitman, J. (2002) Protein kinase A operates a molecular switch that governs yeast pseudohyphal differentiation. *Mol. Cell Biol.* **22,** 3981–3993 CrossRef Medline
75. Lu, P. Y. T., and Kobor, M. S. (2014) Maintenance of heterochromatin boundary and nucleosome composition at promoters by the Asf1 histone chaperone and SWR1-C chromatin remodeler in *Saccharomyces cerevisiae*. *Genetics* **197,** 133–145 CrossRef Medline